



This is a repository copy of *Precision measurement of the B_0 meson lifetime using $B_0 \rightarrow J/\psi K^* 0$ decays with the ATLAS detector*.

White Rose Research Online URL for this paper:

<https://eprints.whiterose.ac.uk/228963/>

Version: Published Version

Article:

Aad, G. orcid.org/0000-0002-6665-4934, Aakvaag, E. orcid.org/0000-0001-7616-1554, Abbott, B. orcid.org/0000-0002-5888-2734 et al. (2927 more authors) (2025) Precision measurement of the B_0 meson lifetime using $B_0 \rightarrow J/\psi K^* 0$ decays with the ATLAS detector. *The European Physical Journal C*, 85 (7). 736. ISSN 1434-6044

<https://doi.org/10.1140/epjc/s10052-025-14232-8>

Reuse

This article is distributed under the terms of the Creative Commons Attribution (CC BY) licence. This licence allows you to distribute, remix, tweak, and build upon the work, even commercially, as long as you credit the authors for the original work. More information and the full terms of the licence here:
<https://creativecommons.org/licenses/>

Takedown

If you consider content in White Rose Research Online to be in breach of UK law, please notify us by emailing eprints@whiterose.ac.uk including the URL of the record and the reason for the withdrawal request.



Precision measurement of the B^0 meson lifetime using $B^0 \rightarrow J/\psi K^{*0}$ decays with the ATLAS detector

ATLAS Collaboration*

CERN, 1211 Geneva 23, Switzerland

Received: 15 November 2024 / Accepted: 27 April 2025
© CERN for the benefit of the ATLAS Collaboration 2025

Abstract A measurement of the B^0 meson lifetime using $B^0 \rightarrow J/\psi K^{*0}$ decays in data from 13 TeV proton–proton collisions with an integrated luminosity of 140 fb^{-1} recorded by the ATLAS detector at the LHC is presented. The measured effective lifetime is

$$\tau = 1.5053 \pm 0.0012 \text{ (stat.)} \pm 0.0035 \text{ (syst.) ps.}$$

The average decay width extracted from the effective lifetime, using parameters from external sources, is

$$\Gamma_d = 0.6639 \pm 0.0005 \text{ (stat.)} \pm 0.0016 \text{ (syst.)} \\ \pm 0.0038 \text{ (ext.) ps}^{-1},$$

where the uncertainties are statistical, systematic and from external sources. The earlier ATLAS measurement of Γ_s in the $B_s^0 \rightarrow J/\psi \phi$ decay was used to derive a value for the ratio of the average decay widths Γ_d and Γ_s for B^0 and B_s^0 mesons respectively, of

$$\frac{\Gamma_d}{\Gamma_s} = 0.9905 \pm 0.0022 \text{ (stat.)} \pm 0.0036 \text{ (syst.)} \pm 0.0057 \text{ (ext.).}$$

The measured lifetime, average decay width and decay width ratio are in agreement with theoretical predictions and with measurements by other experiments. This measurement provides the most precise result of the effective lifetime of the B^0 meson to date.

Contents

| | | |
|-----|---|-------|
| 1 | Introduction | |
| 2 | ATLAS detector, data-taking conditions and simulation | |
| 3 | Event reconstruction and selection | |
| 4 | Maximum-likelihood fit | |
| 4.1 | The invariant mass PDFs | |
| 4.2 | The proper decay time PDFs | |
| 5 | Efficiencies and corrections | |
| 6 | Systematic uncertainties | |

* e-mail: atlas.publications@cern.ch

| | | |
|-----|---|-------|
| 7 | Results | |
| 7.1 | B^0 lifetime result | |
| 7.2 | Determination of the B^0 average decay width Γ_d and the ratio Γ_d/Γ_s | |
| 7.3 | Comparison with other measurements and theory predictions | |
| 8 | Conclusions | |
| | References | |

1 Introduction

The lifetime, or equivalently the decay width, is one of the fundamental properties of elementary particles, and hence it represents an observable of primary phenomenological importance. In particular, studies of b -hadron lifetimes can test our understanding of the weak interaction. On the theoretical side, lifetimes of b -hadrons can be computed systematically in the heavy-quark expansion (HQE) framework [1–8], which permits b -hadron observables to be calculated through perturbative expansion in powers of the reciprocal of the b -quark mass, m_b . The theoretical models typically provide predictions of the ratios of b -hadron lifetimes, since these can be obtained with higher accuracy than is possible for the predictions of absolute lifetimes, due to HQE terms cancelling out in the ratio. Lifetime differences among the b -hadrons are almost entirely attributable to the corrections for Pauli interference and weak annihilation, both of which are enhanced by a relatively large phase space factor where they enter the expansion at the term proportional to m_b^{-3} [9]. This term also includes the non-perturbative matrix of four-quark operators, which was recently calculated [10] using QCD sum rules [11,12] formulated in Heavy Quark Effective Theory (HQET) [13]. The largest contributions to the total uncertainty in the lifetime ratio, as predicted with the HQE, come from the hadronic matrix elements.

The effective lifetime τ_{B^0} is related to the decay widths of the light (L) and heavy (H) mass eigenstates of the $B^0 - \bar{B}^0$

Table 1 Theoretical predictions for the B^0 meson to B_s^0 meson decay width ratio

| Model | Γ_d/Γ_s |
|------------------|---------------------|
| HQE [16] | 1.003 ± 0.006 |
| Lattice QCD [17] | 1.00 ± 0.02 |

system via the following equation taken from Ref. [14]:

$$\tau_{B^0} = \frac{1}{\Gamma_d} \frac{1}{1-y^2} \left(\frac{1+2Ay+y^2}{1+Ay} \right), \quad (1)$$

where $\Gamma_d = (\Gamma_L + \Gamma_H)/2$ is the average decay width of the two states, $y = \Delta\Gamma_d/(2\Gamma_d) = (\Gamma_L - \Gamma_H)/(2\Gamma_d)$ is the normalised width difference, and the asymmetry A depends on the final state f through the following expression:

$$A = \frac{R_H^f - R_L^f}{R_H^f + R_L^f}.$$

Here the amplitudes R_L^f and R_H^f are defined via the summed decay rate of the members of the $B^0 - \bar{B}^0$ system to the final state f , as also given in Ref. [14]:

$$\begin{aligned} \langle \Gamma(B^0(t)) \rangle &= \Gamma(B^0(t)) + \Gamma(\bar{B}^0(t)) \\ &= R_H^f \exp(-\Gamma_H t) + R_L^f \exp(-\Gamma_L t). \end{aligned}$$

Using the values of y and A from Ref. [15], inverting Eq. (1) allows a measured value of Γ_d to be extracted. Its predicted value is $\Gamma_d = 0.63^{+0.11}_{-0.07} \text{ ps}^{-1}$ [16]. Theoretical uncertainties largely cancel out in the decay width ratio Γ_d/Γ_s , where Γ_s is average B_s^0 meson decay width. Table 1 lists the decay width ratios of B^0 and B_s^0 mesons as predicted by the HQE model in Ref. [16] and the lattice QCD model in Ref. [17].

Previous measurements of the B^0 meson lifetime have been reported by a variety of collaborations. For the LHC experiments, these are ATLAS [18], LHCb [19, 20] and CMS [21]. The most recent result comes from Belle II [22]. Other measurements were performed by BaBar [23], CDF [24], D0 [25] and Belle [26].

This article reports a measurement of the effective lifetime of the B^0 meson by the ATLAS experiment. Data amounting to 140 fb^{-1} of $\sqrt{s} = 13 \text{ TeV}$ proton–proton (pp) collisions were collected at the CERN Large Hadron Collider (LHC) during the period 2015–2018. The B^0 is identified using its decay mode $B^0 \rightarrow J/\psi K^{*0}(892)$ with $J/\psi \rightarrow \mu^+ \mu^-$ and $K^{*0}(892) \rightarrow K^+ \pi^-$. Inclusion of conjugate modes is implied unless noted otherwise. A combined analysis of the mass and lifetime distributions is performed, where the mass is used to improve discrimination between the signal and background.

The average decay width Γ_d and the ratio of widths Γ_d/Γ_s , using the ATLAS-measured value of Γ_s [27], are also determined in this analysis. Values of y and A used to extract Γ_d are taken from Ref. [15].

2 ATLAS detector, data-taking conditions and simulation

The ATLAS detector¹ [28] consists of three main components: an inner detector (ID) tracking system immersed in a 2 T axial magnetic field, electromagnetic and hadronic calorimeters, and a muon spectrometer (MS). The ID covers the pseudorapidity range $|\eta| < 2.5$ and consists of silicon pixel, silicon microstrip, and transition radiation tracking detectors [29]. The first point of detection is the insertable B-layer at a radius of 3.3 cm from the beam line; the rest of the pixel detector consists of 92 million pixels capable of measuring the location of a hit to a precision of $10 \mu\text{m}$ [30, 31]. It is surrounded by the silicon microstrip detector, which consists of 6 million microstrip sensors. The ID is surrounded by a high-granularity liquid-argon (LAr) sampling electromagnetic calorimeter. A steel/scintillator tile calorimeter provides hadronic coverage in the central rapidity range. The endcap and forward regions are equipped with LAr calorimeters for electromagnetic and hadronic measurements. The MS surrounds the calorimeters. It comprises separate trigger and high-precision tracking chambers measuring the deflection of muons in a magnetic field generated by superconducting air-core toroids. The field integral of the toroids ranges between 2.0 and 6.0 Tm across most of the detector. A set of precision chambers covers the region $|\eta| < 2.7$ with three layers of monitored drift tubes, complemented by cathode strip chambers in the forward region, where the background is highest. The muon trigger system covers the range $|\eta| < 2.4$ with resistive plate chambers in the barrel, and thin gap chambers in the endcap regions. The luminosity is measured mainly by the LUCID-2 [32] detector that records Cherenkov light produced in the quartz windows of photomultipliers located close to the beampipe.

Events are selected by the first-level trigger system implemented in custom hardware, followed by selections made by algorithms implemented in software in the high-level trigger [33]. The first-level trigger accepts events from the 40 MHz bunch crossings at a rate below 100 kHz, which the

¹ ATLAS uses a right-handed coordinate system with its origin at the nominal interaction point. The z -axis is along the beam pipe, the x -axis points to the centre of the LHC ring, and the y -axis points upward. Cylindrical coordinates (r, ϕ) are used in the transverse plane, r being the distance from the origin and ϕ being the azimuthal angle around the beam pipe. The pseudorapidity η is defined as $\eta = -\ln[\tan(\theta/2)]$ where θ is the polar angle.

high-level trigger further reduces in order to record complete events to disk at about 1 kHz.

The data were collected during periods with different instantaneous luminosities, so several triggers were used in the analysis [34, 35]. All triggers were based on the identification of a $J/\psi \rightarrow \mu^+ \mu^-$ decay, with various muon transverse momentum (p_T) thresholds (usually 4 GeV, 6 GeV and 11 GeV). The composition of the collected data shifts to higher thresholds as the number of pp interactions per bunch crossing (pile-up) increases. Data quality requirements are imposed on the data, notably on the performance of the MS, ID and calorimeter systems [36]. The measurement uses pp collision data corresponding to an integrated luminosity of $140.1 \pm 1.2 \text{ fb}^{-1}$ [37], a value obtained by the LUCID-2 detector [32] for the primary luminosity measurements. An extensive software suite [38] is used in data simulation, in the reconstruction and analysis of real and simulated data, in detector operations, and in the trigger and data acquisition systems of the experiment.

To model the $B^0 \rightarrow J/\psi K^{*0}$ decay in the ATLAS detector, a Monte Carlo (MC) simulated sample of signal events was generated. These events were required to have at least one pair of oppositely charged muons with $p_T > 3.5 \text{ GeV}$ and $|\eta| < 2.6$ to match the fiducial acceptance of the detector. Production of b -hadrons in pp collisions was simulated using PYTHIA 8.244 [39], tuned to ATLAS data via the A14 set of tuned parameters [40], together with the CTEQ6L1 set of parton distribution functions [41]. The MC events were then passed through the ATLAS detector simulation program based on the ATLFAST2 procedure [42] using the GEANT4 package [43]. The same software as used for processing data from the detector was also used to reconstruct the simulated events. The MC events were weighted to reproduce the same pile-up, and the same trigger conditions as in the data, including the pre-scale factors² applied in data-taking.

3 Event reconstruction and selection

Events are first required to pass the trigger selections described in Sect. 2. In addition, each event must contain at least one reconstructed primary vertex [44], formed from at least four ID tracks, and at least one pair of oppositely charged muon candidates that are reconstructed using information from the MS and the ID. The muons used in the analysis are required to meet the *Tight* working point identification criteria [45]. The oppositely charged muon pairs are re-fitted to a common vertex (using ID track parameters only), and the pair is accepted if the quality of the fit meets the requirement $\chi^2/\text{ndof} < 10$ for its reduced χ^2 value. Here,

ndof represents the number of degrees of freedom. Additionally, the J/ψ mass, extracted in the fit, must lie within a range selected to retain 99.7% of the J/ψ candidates identified in the fits. The size of the chosen range depends on the pseudo-rapidity of the muons. The $K^{*0} \rightarrow K^+ \pi^-$ decay candidates are reconstructed from all tracks that are not identified as muons from the J/ψ decay. The oppositely charged tracks are reconstructed under both the K^{*0} and \bar{K}^{*0} hypotheses, and the hypothesis giving an invariant mass closer to the world average value for the K^* meson is selected. Selected tracks satisfying $p_T(K^+) > 1 \text{ GeV}$, $p_T(\pi^-) > 0.5 \text{ GeV}$ and $|\eta| < 2.5$ are used, and the $K^{*0} \rightarrow K^+ \pi^-$ candidate is required to satisfy $p_T(K^{*0}) > 3.5 \text{ GeV}$ and lie in the range $846 \text{ MeV} < m(K^+ \pi^-) < 946 \text{ MeV}$.

Each combination of the selected $J/\psi \rightarrow \mu^+ \mu^-$ and $K^{*0} \rightarrow K^+ \pi^-$ candidates is fitted to a common vertex, forming the $B^0 \rightarrow J/\psi K^{*0}$ candidates. The vertex fit is constrained by fixing the invariant mass of the two muon tracks to the world average value of the J/ψ mass [46]. The $B^0 \rightarrow J/\psi K^{*0}$ candidates that fulfil a $\chi^2/\text{ndof} < 3$ condition are accepted for further analysis. The B^0 candidate with the lowest χ^2/ndof is selected in events with more than one candidate meeting the criteria. In total, 10 559 554 B^0 candidates are selected within the mass range 5.00–5.65 GeV. This range is chosen so that the sidebands of the mass distribution have enough background events to allow a precise determination of their properties.

The mean number of pp interactions per bunch crossing is 31, so it is necessary to choose the best candidate for the primary vertex at which the B^0 meson is produced. Primary vertex (PV) positions are recalculated after removing any tracks used in the B^0 meson reconstruction. The PV candidate with the smallest three-dimensional impact parameter, a_0 (the minimum distance between each PV candidate and the line extrapolated from the reconstructed B^0 meson vertex in the direction of the B^0 momentum), is used. For each B^0 meson candidate, the proper decay time t is determined using:

$$t = \frac{L_{xy} m_B}{p_{T_B}}, \quad (2)$$

where p_{T_B} is the reconstructed transverse momentum of the B^0 meson candidate and m_B denotes the mass of the B^0 meson, taken from Ref. [46]. The transverse decay length, L_{xy} , is the distance in the transverse plane from the primary vertex to the B^0 meson decay vertex, projected onto the direction of the B^0 transverse momentum.

² A pre-scale factor defines the fraction of events that are kept from all those that would have passed the trigger requirements.

4 Maximum-likelihood fit

The lifetime of the B^0 meson is extracted from a two-dimensional unbinned maximum-likelihood fit describing both signal and background. The signal model describes the $B^0 \rightarrow J/\psi K^{*0}$ decay events. The background model is composed of two contributions. The first one, referred to as ‘prompt’ background, corresponds to cases where the J/ψ meson coming from the $pp \rightarrow J/\psi X$ production process is combined with a random K^{*0} candidate in the same event. The other contribution, referred to as ‘combinatorial’ background, is formed of events where a J/ψ meson produced in the decay of any b -hadron is combined with a K^{*0} candidate.

The mass and proper decay time are simultaneously fitted using the log-likelihood function:

$$\ln L = \sum_{i=1}^N w(t_i) \ln [f_{\text{sig}} \mathcal{M}_{\text{sig}}(m_i) \mathcal{T}_{\text{sig}}(t_i, \sigma_{t_i}, p_{T_i}) + (1 - f_{\text{sig}}) \mathcal{M}_{\text{bkg}}(m_i) \mathcal{T}_{\text{bkg}}(t_i, \sigma_{t_i}, p_{T_i})],$$

where f_{sig} is the fraction of signal events in the total number of events, N . The $B^0 \rightarrow J/\psi K^{*0}$ decay is described by the mass probability density function (PDF) \mathcal{M}_{sig} multiplied by the time PDF \mathcal{T}_{sig} . The prompt and combinatorial backgrounds are modelled by the mass and lifetime PDFs \mathcal{M}_{bkg} and \mathcal{T}_{bkg} . The mass m_i , the proper decay time t_i , its uncertainty σ_{t_i} and the B^0 candidate transverse momentum p_{T_i} are the values measured from the data for each event i . The weight $w(t_i)$, as defined by Eq. (6) in Sect. 5, accounts for the selection efficiency.

4.1 The invariant mass PDFs

The \mathcal{M}_{sig} and \mathcal{M}_{bkg} PDFs model the B^0 signal and background mass shapes, respectively, in the fitted mass range. For the signal, the mass is modelled with a Johnson S_U -distribution [47]:

$$\mathcal{M}_{\text{sig}}(m_i) = \frac{\delta}{\lambda \sqrt{2\pi} \sqrt{1 + \left(\frac{m_i - \mu}{\lambda}\right)^2}} \times \exp \left[-\frac{1}{2} \left(\gamma + \delta \sinh^{-1} \left(\frac{m_i - \mu}{\lambda} \right) \right)^2 \right],$$

where μ , γ , δ and λ are free parameters. For the background, the mass distribution is modelled by the sum of a polynomial and a sigmoid function:

$$\mathcal{M}_{\text{bkg}}(m_i) = f_{\text{poly}}(1 + p_0 \cdot m_i) + (1 - f_{\text{poly}}) \times \left(1 - \frac{s(m_i - m_0)}{\sqrt{1 + (s(m_i - m_0))^2}} \right), \quad (3)$$

where f_{poly} describes the relative size of the two components and m_0 , s and p_0 are parameters of the PDF. Here the sigmoid function was added to better describe the background contribution from partially reconstructed B mesons in the lower-mass sideband.

4.2 The proper decay time PDFs

The PDF describing the proper decay time for each event i is composed of two terms:

$$\mathcal{T}_j(t_i, \sigma_{t_i}, p_{T_i}) = P_j(t_i | \sigma_{t_i}, p_{T_i}) \cdot C_j(\sigma_{t_i}, p_{T_i}), \quad (4)$$

where $j \in (\text{sig}, \text{bkg})$ stands for signal or background, respectively. In each term P_j the function describing the proper decay time behaviour of component j is convolved with the proper decay time resolution function in order to account for the proper decay time uncertainty. The resolution function is modelled as a sum of three Gaussian distributions:

$$R(t' - t_i, \sigma_{t_i}) = \sum_{k=1}^3 f_{\text{res}}^{(k)} \frac{1}{\sqrt{2\pi} S^{(k)} \sigma_{t_i}} \exp \left(\frac{-(t' - t_i)^2}{2(S^{(k)} \sigma_{t_i})^2} \right).$$

The scale factors $S^{(k)}$ are free parameters of the fit. The value of σ_{t_i} is the per-candidate uncertainty in t_i , extracted from the vertex fit performed for the $B^0 \rightarrow J/\psi K^{*0}$ candidate, described in Sect. 3. The parameters $f_{\text{res}}^{(k)}$ represent the relative contribution of each Gaussian function and fulfil the normalization condition $\sum f_{\text{res}}^{(k)} = 1$.

The signal proper decay time distribution of the B^0 signal candidates is modelled as an exponential function

$$P_{\text{sig}}(t_i | \sigma_{t_i}, p_{T_i}) = E(t', \tau_{B^0}) \otimes R(t' - t_i, \sigma_{t_i}),$$

where $E(t, \tau_{B^0}) = (1/\tau_{B^0}) \exp(-t/\tau_{B^0})$ for $t \geq 0$, with the parameter τ_{B^0} standing for the B^0 lifetime.

The proper decay time PDF for the background candidates, P_{bkg} , consists of two parts. One part accounts for the prompt background and consists of the resolution function R only. The other part accounts for the combinatorial background and consists of a sum of three exponential functions, each convolved with the resolution function R . In summary, the background proper decay time PDF takes the form:

$$P_{\text{bkg}}(t_i | \sigma_{t_i}, p_{T_i}) = \left(f_{\text{prompt}} \cdot \delta_{\text{Dirac}}(t') + (1 - f_{\text{prompt}}) \sum_{k=1}^3 b_k \prod_{l=1}^{k-1} (1 - b_l) E(t', \tau_{\text{bkg}_k}) \right) \otimes R(t' - t_i, \sigma_{t_i}). \quad (5)$$

Here the τ_{bkg_j} are different lifetimes describing three components of the combinatorial background; the parameters b_j are

the relative fractions of these three background components, and f_{prompt} is the prompt component's fraction. Parameters τ_{bkg_j} , f_{prompt} and two of the b_j are free in the fit; $b_3 \equiv 1$ by definition.

The probability terms $C_j(\sigma_{t_i}, p_{T_i})$ in Eq. (4) are two-dimensional distributions introduced to describe the difference between signal and background for the per-candidate time uncertainty σ_{t_i} and p_{T_i} values, respectively [48]. The distributions of σ_{t_i} for signal and background are extracted from the data using the *sPlot* technique [49] with the B^0 candidate mass as the discriminating variable.

5 Efficiencies and corrections

The trigger, offline reconstruction, and event selection criteria bias the reconstructed proper-decay time distribution. These effects are estimated using signal MC events. The triggers used in this analysis impose no lower threshold on either the transverse impact parameter d_0 of each muon or on the displacement of the J/ψ vertex. The same is true for the offline tracking and event selections. On the other hand, both the trigger and offline tracking impose an upper limit on $|d_0|$, namely $|d_0| < 10$ mm, for all four final-state tracks from a $B^0 \rightarrow J/\psi K^{*0}$ decay. This results in inefficiency at large values of the proper decay time.

To study inefficiency effects, the signal MC events generated in the fiducial volume of the ATLAS detector, with no selection applied to the final-state particles from $B^0 \rightarrow J/\psi K^{*0}$ decays, are used. Subsequently, these events are passed through a simulation of the detector response and triggers, followed by offline tracking and vertexing algorithms. This procedure includes magnetic field simulation, tracking efficiency calibration, and trigger pre-scale emulations to ensure a consistency with data. Finally, the event selection criteria listed in Sect. 3 are applied. The B^0 proper decay time distributions obtained before and after the whole chain are used to estimate time inefficiencies for each year of data-taking. To account for these inefficiencies in the fit, each event i is weighted by a factor w_i , which is inversely proportional to the time efficiency function and is defined as:

$$1/w_i(t_i) = p_0 \cdot [1 - p_1 \cdot (\text{Erf}((t_i - p_3)/p_2) + 1)]. \quad (6)$$

Here ‘Erf’ denotes the error function, and the values of parameters p_0 , p_1 , p_2 and p_3 are determined in the fit to the MC events. The fit is applied individually for each year, due to their different trigger and data-taking conditions. Since the analysis is not sensitive to the absolute value of the efficiency, only corrections to the shape of the time efficiency functions are applied. Thus the overall normalisation parameter p_0 is chosen to have a weight equal to unity on average for each

Table 2 Summary of systematic uncertainties assigned to the value of the B^0 lifetime

| Source of uncertainty | Systematic uncertainty [ps] |
|--|-----------------------------|
| ID alignment | 0.00108 |
| Choice of mass window | 0.00104 |
| Time efficiency | 0.00135 |
| Best-candidate selection | 0.00041 |
| Mass fit model | 0.00152 |
| Mass-time correlation | 0.00229 |
| Proper decay time fit model | 0.00010 |
| Conditional probability model | 0.00070 |
| Fit model test with pseudo-experiments | 0.00002 |
| Total | 0.0035 |

year of data-taking. The systematic uncertainties associated with the time efficiency determination and its application in data correction are explained in the Sect. 6 and included in the systematic uncertainties of the measurement.

6 Systematic uncertainties

The systematic uncertainties in the B^0 lifetime arise from several sources. The uncertainties are estimated from comparisons of nominal and modified fit results and from observed fit biases in modified pseudo-experiments. The statistical uncertainty of the default fit is $\sigma_{\text{stat}} = 0.0012$ ps. A summary of all sources of uncertainty that contribute to the analysis is presented in Table 2, where the total systematic uncertainty is obtained by adding all of the contributions in quadrature. Each of the systematic uncertainties is described below.

- **Inner detector alignment:** Effects due to the ATLAS ID misalignment are dominated by the global length scale biases. These are characterised by detector geometry distortions along the track trajectory and affect both the radial and longitudinal directions, causing biases to the measured transverse and longitudinal momenta [50]. This effect manifests itself as a shift in the reconstructed invariant mass of known resonances. ATLAS determined that the global length bias equally affects both radius and length of detector leading to momenta biases: $p'_T = p_T(1 + \epsilon_s)$ and $p'_Z = p_Z(1 + \epsilon_s)$, where ϵ_s is a scale factor. On the basis of $J/\psi \rightarrow \mu^+\mu^-$ events the scale $\epsilon_s = -0.085\%$ has been determined. The value is consistent with the one extracted for $Z \rightarrow \mu^+\mu^-$ in the same paper [50].

In this analysis the tracks forming the B^0 candidate vertex are re-fitted with the J/ψ candidate mass constrained

to the world average value, effectively removing the misalignment effect from the data. The impact of the ID misalignment in the lifetime determination is estimated by performing an alternative fit, where the tracks forming the B^0 meson vertex are re-fitted without constraining the J/ψ mass to its world average value. It is worth noting that the measurement of the momentum bias, using invariant mass of resonances [50], involving radial and longitudinal scale length biases, also includes momentum biases due to magnetic field distortions. The proper decay time in this analysis is calculated using the ratio of L_{xy} and p_{T_B} with Eq. (2). The value of L_{xy} is sensitive to the radial length scale bias in the same way as p_{T_B} , while L_{xy} is not sensitive to the magnetic field distortions. So in the proper decay time, the misalignment effects only partially cancel. To follow a conservative approach, the alternative fit without a J/ψ mass constraint was performed and compared to the default fit that includes J/ψ constraint, resulting in a difference $0.9\sigma_{\text{stat}}$ of the B^0 lifetimes, which is included into systematic uncertainty due to misalignment. Additionally, to account for the momentum scale bias affecting low- p_T hadrons, the p_T values of hadrons from the K^{*0} decay are altered by -0.085% [50]. The difference of lifetimes between this alternative fit and the default one is conservatively taken as a systematic uncertainty associated with the momentum bias of the low- p_T hadrons due to ID misalignment. The two effects have been symmetrised and summed in quadrature, giving the value of $1.0\sigma_{\text{stat}}$, that serves as an estimate for the total systematic uncertainty due to ID misalignment.

- **Choice of mass window:** The sensitivity of the lifetime fit to the chosen B^0 mass window is estimated by choosing other intervals as alternatives to the default mass range of 5000–5650 MeV. Several other intervals are studied, varying the mass range limits by ± 20 MeV or ± 40 MeV. The largest deviation of the alternative fit lifetimes from the default value, $0.9\sigma_{\text{stat}}$, is taken as an estimate of this systematic uncertainty.
- **Choice of primary vertex:** As mentioned in Sect. 3, among the multiple primary vertices typically found in an event, the PV with the smallest a_0 is chosen by default. An alternative approach is to use the PV with the highest sum of the squares of the constituent tracks' transverse momenta, $\sum p_T^2$. The difference between the B^0 fitted lifetimes obtained using the default and alternative approaches is negligibly small compared to the statistical uncertainty of the fit. The small difference is due to the fact that the PV position resolution in the transverse plane is same as the beam-spot size. A PV position difference in the z -direction is not relevant, since the lifetime is extracted in the transverse plane, as defined in Eq. (2).

- **Time efficiency:** Time efficiency curves are used to correct for the proper decay time dependence of reconstruction, trigger and candidate selection inefficiencies. They are built with information from MC events, as is described in Sect. 5. Two alternative time efficiency functions are obtained by replacing the error function in Eq. (6) with either a hyperbolic tangent function or $(x^2 + 1)^{-1/2}$. The larger of the changes in the fitted lifetime, of size $0.6\sigma_{\text{stat}}$, is taken as a systematic uncertainty. To account for potential systematic effects due to the limited MC sample size, a large number of alternative time efficiency functions are obtained by smearing the number of MC events in the time bins used to determine the time efficiency function. These functions are then used to rerun the unbinned maximum-likelihood fit on the data. The set of these fit results is characterized by its mean value and standard deviation, and these contribute a systematic uncertainty of $0.8\sigma_{\text{stat}}$. An alternative fit using data events satisfying the requirement $t < 8$ ps, where the efficiency is almost constant, is performed to validate the modelling of the efficiency dependence on the lifetime for high lifetimes, where the efficiency decrease is large. This systematic test examines associated effects, such as modelling of tracking efficiencies, triggers, variations in the magnetic field, and provides a conservative estimate of their uncertainties. The systematic uncertainty derived from this test is $0.5\sigma_{\text{stat}}$. Choosing a somewhat different upper requirement on t has minimal impact on the test results. Another test is performed by building alternative time efficiency functions based on a signal MC with helicity angles shaped according to full PDF of $B^0 \rightarrow J/\psi K^{*0}$ measured by LHCb [51]. The resulting lifetime is identical with the default one within $0.3\sigma_{\text{stat}}$. All contributions to the systematic uncertainty associated with the time efficiency are added in quadrature.
- **Best-candidate selection:** 90% of events that meet all the selection criteria (listed in Sect. 3) contain just one B^0 meson candidate. The others have 2.1 candidates on average. These were all found to share the same J/ψ in their event. Only the candidate with the lowest χ^2/ndof in the event is retained for the analysis. The systematic uncertainty due to candidate selection is estimated by applying an alternative time efficiency curve calculated from MC events by using the true generated candidates instead of the lowest χ^2/ndof candidate. The systematic uncertainty estimated from this test is $0.3\sigma_{\text{stat}}$. Both efficiency functions, based on different candidate selection criteria, were validated on signal MC events, reproducing the lifetime value with a precision well below the statistical uncertainty.
- **Mass fit model:** To estimate how mismodelling of the mass distribution affects the fitted B^0 lifetime, three contributions are considered. The first contribu-

tion comes from kinematic reflections, where one of the tracks is either misidentified as another particle or completely missing. The MC simulation is used to model the shapes of the kinematic reflections, and four channels that are non negligible, $B^+ \rightarrow J/\psi K^+$, $B_s^0 \rightarrow J/\psi K^{*0}(K^-\pi^+)$, $B_s^0 \rightarrow J/\psi K^+ K^-$ and $B^0 \rightarrow J/\psi \rho(\pi^+\pi^-)$ (with intermediate ϕ and ρ^0 resonances accounted for in the last two channels), are included in the fit to data with freely floating relative fractions, while the lifetimes are shaped same as the combinatorial background. Contributions of the various channels are included either individually or together. These alternative fits result in the B^0 lifetime values that differ from the nominal one by up to $1.0\sigma_{\text{stat}}$. For the $B_s^0 \rightarrow J/\psi K^{*0}(K^-\pi^+)$ decay contribution, the signal-like lifetime model was also tested by fixing the lifetime to the B_s^0 flavor-specific world average value [46], producing results consistent with the fit that modeled the lifetime distribution as the combinatorial background across all four channels. Other channels like $\Lambda_b \rightarrow J/\psi K p$, $\Lambda_b \rightarrow J/\psi \Lambda^0$ and $\Lambda_b \rightarrow J/\psi p\pi^-$ are found to be negligible. The resulting deviation from the default fit's B^0 lifetime value is used as a systematic uncertainty. Secondly, the signal mass is tested by running alternative fits with different signal mass models, where the Johnson S_U -distribution in Eq. (3) is replaced by a double-sided Crystal Ball distribution [52] or Student's t -distribution [53]. The maximum deviation from the default fit is included in the systematic uncertainty. Lastly, the systematic uncertainty from the choice of background mass PDF is estimated by using alternative functions where the sigmoid component of Eq. (3) is replaced by either an arctan function or $(1 + |s(m_i - m_0)|)^{-1}$. Systematic deviations from all the variations described above, added in quadrature give a systematic error of $1.3\sigma_{\text{stat}}$ and they are included in the total systematic uncertainty.

- **Mass-time correlation:** The correlations between the invariant mass and the pseudo-proper decay time, and their potential impact on the fit results, is studied. For the signal events the MC simulation shows a negligible correlation between these two variables. A data driven method is used for background events, the mass-sideband regions $5.000 \text{ GeV} < m_B < 5.100 \text{ GeV}$ (left) and $5.450 \text{ GeV} < m_B < 5.650 \text{ GeV}$ (right) are divided into six bins of equal size of 50 MeV. Then using the lifetime background description of the default PDF function, Eq. (5), the component fractions f_{prompt} , b_1 , and b_2 are determined through likelihood fits for each of the six mass bins. These values are found to be linearly dependent on the mass. An alternative PDF is then constructed in the mass-lifetime fit with $f_{\text{prompt}}(m_i) = a + b(m_i - 5.279 \text{ GeV})$, $b_1(m_i) = c_1 + d_1(m_i - 5.279 \text{ GeV})$ and $b_2(m_i) = c_2 + d_2(m_i - 5.279 \text{ GeV})$, where $a, b, c_1, d_1,$

c_2 and d_2 are free parameters of the fit. These are found to be consistent with the linear dependency observed in the mass-sideband bins. This alternative fit results in the B^0 lifetime value, that is by $1.9\sigma_{\text{stat}}$ different from the default one. This difference is taken as a systematic uncertainty of the fit due to mass-time correlation.

- **Proper decay time fit model:** The proper decay time resolution model is a sum of three Gaussian distributions with a common mean at zero and freely floating relative fractions. Alternative resolution models employing two or four Gaussian functions were evaluated. The impact of choosing the three-Gaussian resolution model instead of an alternative one is treated as a systematic uncertainty. The decay time probability density function for background events is constructed by combining three exponential functions. The use of this model is validated by examining events gathered from the invariant mass sidebands. An alternative model with four exponential functions was tested, resulting in negligible systematic uncertainty.
- **Conditional probability model:** The probability terms $C_j(\sigma_{t_i}, p_{T_i})$ in Eq. (4) are two-dimensional distributions introduced to describe differences between signal and background events with regard to their per-candidate time uncertainties σ_{t_i} and p_{T_i} values. One source of systematic uncertainty is the binning choice. Another source is the choice of method used to smooth the binned distribution. The default model uses a kernel smoothing method based on Gaussian smearing with variable width to cope with zero-content bins, and additional interpolation between bins is performed as a systematic test. The systematic uncertainty in the B^0 lifetime from these sources is evaluated as the maximum deviation from the nominal fit result when combining the variations described above, and is found to be $0.5\sigma_{\text{stat}}$. An additional test was conducted to assess the impact of using Punzi distributions derived from the same dataset, where the dataset was split into halves and a Punzi distribution was extracted from the second half. The observed difference of $0.3\sigma_{\text{stat}}$ between the fit results using the Punzi distribution from the original dataset and the one from the second half is incorporated into the total systematic uncertainty in quadrature.
- **Fit model test with pseudo-experiments:** The fit model can be sensitive to some of the nuisance parameters (e.g. parameters modelling the mass and background lifetime distribution shapes), which could potentially lead to a bias in the measured physics parameters, even if the model describes the fitted data well. The nominal fit model, with its parameter values extracted from the fit to data, was used to generate an ensemble of pseudo-experiments, which were subsequently fitted with the same model. The mean deviation of the B^0 lifetime val-

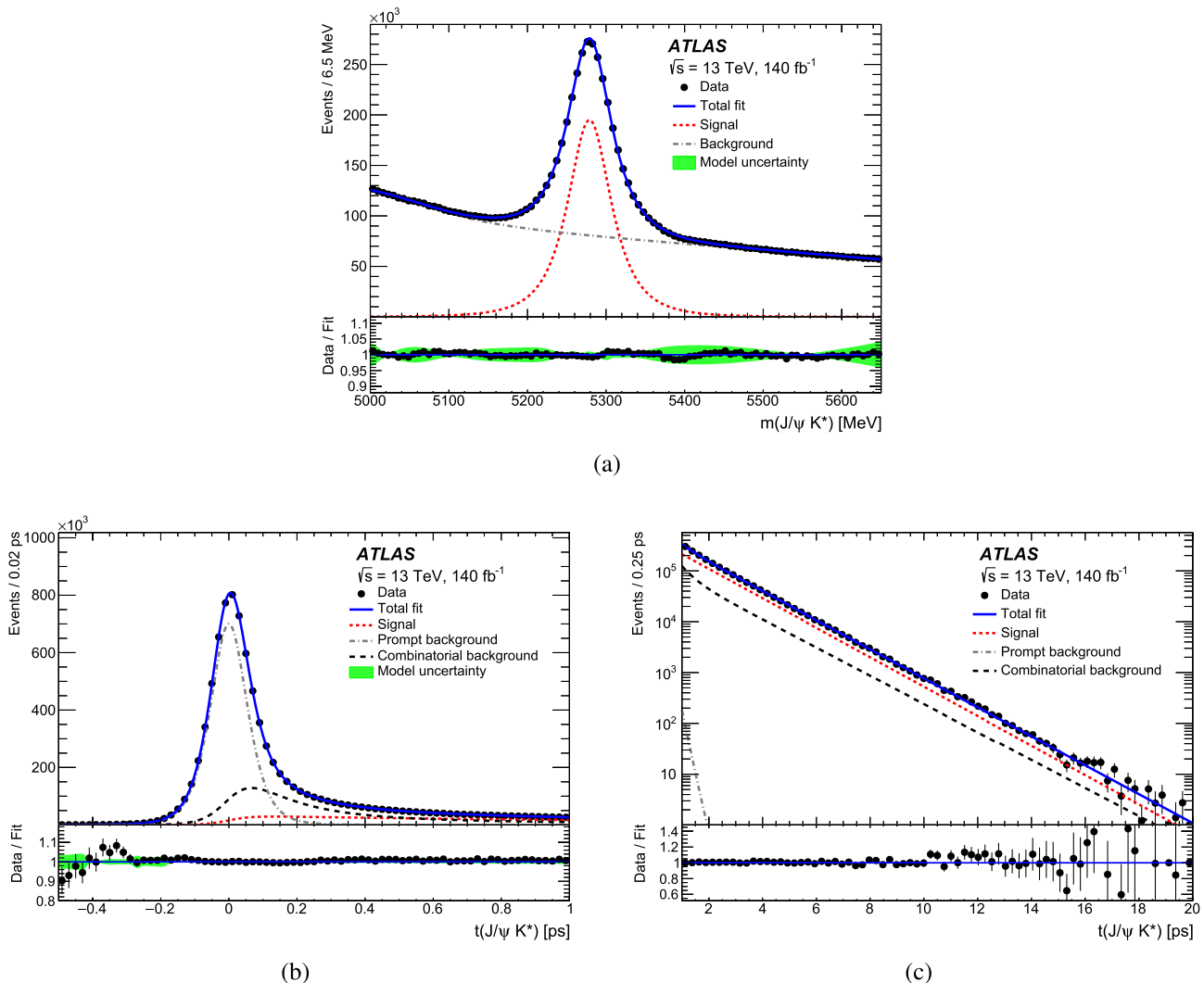


Fig. 1 **a** Invariant mass fit projection and proper decay time fit projection for the $B^0 \rightarrow J/\psi K^{*0}$ sample shown in two different proper decay time ranges: **b** $t \in (-0.5; 1.0)$ ps and **c** $t \in (1; 20)$ ps. The solid blue line shows the total fit while the short-dashed red line shows the signal. The sum of prompt and combinatorial backgrounds in the mass fit projection is represented by the dash-dotted grey line. The lifetime projections show the prompt background as a dash-dotted grey line and

the combinatorial background as a long-dashed black line. The lower panel of each figure shows the ratio of each data point to the total fitted value. The green band in the ratio plot represents the envelope of model variations included in the systematic uncertainty, while the bars on the data points indicate statistical uncertainties. In subfigure **c**, the model variation band is too small to be visible

ues extracted from the pseudo-experiment fits is assigned as a systematic uncertainty.

The systematic uncertainties listed in Table 2 are treated as uncorrelated and thus added in quadrature.

Various tests are done to confirm the stability of the results across trigger selections and B^0 candidate p_T range. The data sample is divided according to three categories of triggers, based on the muon p_T thresholds used in the trigger algorithms. Additionally, three subsamples are created by splitting into three p_T ranges with similar data statistics. In both cases, the resulting B^0 lifetime value remains consistent with the full dataset fit.

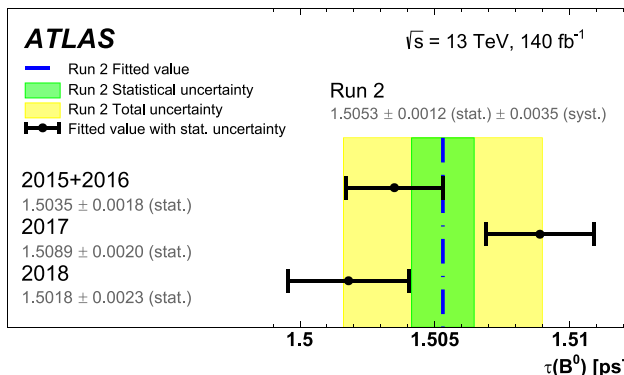


Fig. 2 The fitted values of the B^0 lifetime, measured with $B^0 \rightarrow J/\psi K^{*0}$ decays, for the 2015+2016, 2017 and 2018 subsamples compared to the value for the whole sample. The B^0 lifetime value for each subsample is shown by a black point, with the error bar indicating the statistical uncertainty

7 Results

7.1 B^0 lifetime result

The B^0 effective lifetime value measured with a total of $2\,450\,500 \pm 2400$ B^0 signal events³ is found to be

$$\tau_{B^0} = 1.5053 \pm 0.0012 \text{ (stat.)} \pm 0.0035 \text{ (syst.) ps.} \quad (7)$$

The invariant mass and lifetime projections of the two-dimensional maximum-likelihood fit are shown in Fig. 1. The lower panels show the ratio of each data point to the fitted value and, for the top figure only, a band that represents the envelope of mass fit model variations included in the systematic uncertainty.

As a consistency and stability test, the B^0 lifetime value was fitted separately for each data-taking period (2015+2016, 2017 and 2018). Figure 2 shows the degree of stability over time. The p -value for consistency of the three individual results, accounting for statistical uncertainties only, is 0.038.

7.2 Determination of the B^0 average decay width Γ_d and the ratio Γ_d/Γ_s

Equation (1) is used to extract the average decay width Γ_d from the measured effective lifetime τ_{B^0} . The value of $2y = \Delta\Gamma_d/\Gamma_d = 0.001 \pm 0.010$ is taken from the combination of measurements by HFLAV [15]. The production rate asymmetry $A = -0.578 \pm 0.136$ is calculated from the polarization amplitudes [15]. Using the values of y , A and

the fitted B^0 lifetime, the average decay width is

$$\Gamma_d = 0.6639 \pm 0.0005 \text{ (stat.)} \pm 0.0016 \text{ (syst.)} \\ \pm 0.0038 \text{ (ext.) ps}^{-1}.$$

The uncertainty originating from the external HFLAV uncertainties (denoted ‘ext.’) is given separately. It is calculated from the uncertainties in the values of y and A , and it dominates the overall uncertainty.

The ratio of the average decay widths of the B^0 and B_s^0 mesons, Γ_d/Γ_s , is another quantity of interest in this analysis. The average decay width Γ_s was measured previously by the ATLAS Collaboration [27] as $\Gamma_s = 0.6703 \pm 0.0014 \text{ (stat.)} \pm 0.0018 \text{ (syst.) ps}^{-1}$. The resulting ratio is

$$\frac{\Gamma_d}{\Gamma_s} = 0.9905 \pm 0.0022 \text{ (stat.)} \pm 0.0036 \text{ (syst.)} \pm 0.0057 \text{ (ext.)},$$

where the statistical, systematic and external uncertainties are propagated from the quantities above. In the ratio Γ_d/Γ_s the systematic uncertainties of the ATLAS measurements of τ_{B^0} and Γ_s primarily come from different sources. They are therefore treated as uncorrelated and can simply be added in quadrature.

7.3 Comparison with other measurements and theory predictions

A comparison of the current B^0 lifetime result with the latest and most precise results from other experiments is shown in Fig. 3. This result is compatible with most of the other measurements. In the case of LHCb, three precise measurements are quoted, each of them in a different channel. The one in the $B^0 \rightarrow J/\psi K_S^0$ channel agrees with the ATLAS result. In each of the following comparisons, the quantity σ is estimated by combining the uncertainties from ATLAS and the other source. Thus, the other two LHCb results have lifetimes larger than the current ATLAS value by 2.3σ in $B^0 \rightarrow J/\psi K^{*0}$ and 1.5σ in $B^0 \rightarrow K^+\pi^-$. The latest world average measured value, published in 2024, is 1.517 ± 0.004 ps [46], which differs from this measurement by 2.1σ . This value includes all results obtained in the history of B^0 lifetime measurements.

Compared to the previous ATLAS measurement [18] at $\sqrt{s} = 7$ TeV, the new ATLAS measurement reduces the systematic uncertainty by a factor of 4.7. Although the previous measurement was based on $B^0 \rightarrow J/\psi K_S^0$, which typically has larger systematic uncertainties because of the longer-lived K_S^0 , much of the improvement comes from the insertable B-layer installed in ATLAS after Run 1, which provides more precise vertexing and hence better time resolution. Furthermore, better ID alignment in Run 2 than in Run 1 allowed the related systematic uncertainties to be reduced. In addition, the larger dataset recorded in Run 2 allowed more

³ The number of signal events is calculated from the total number of event candidates and the signal fraction value of 0.23175 ± 0.00022 obtained by the fit.

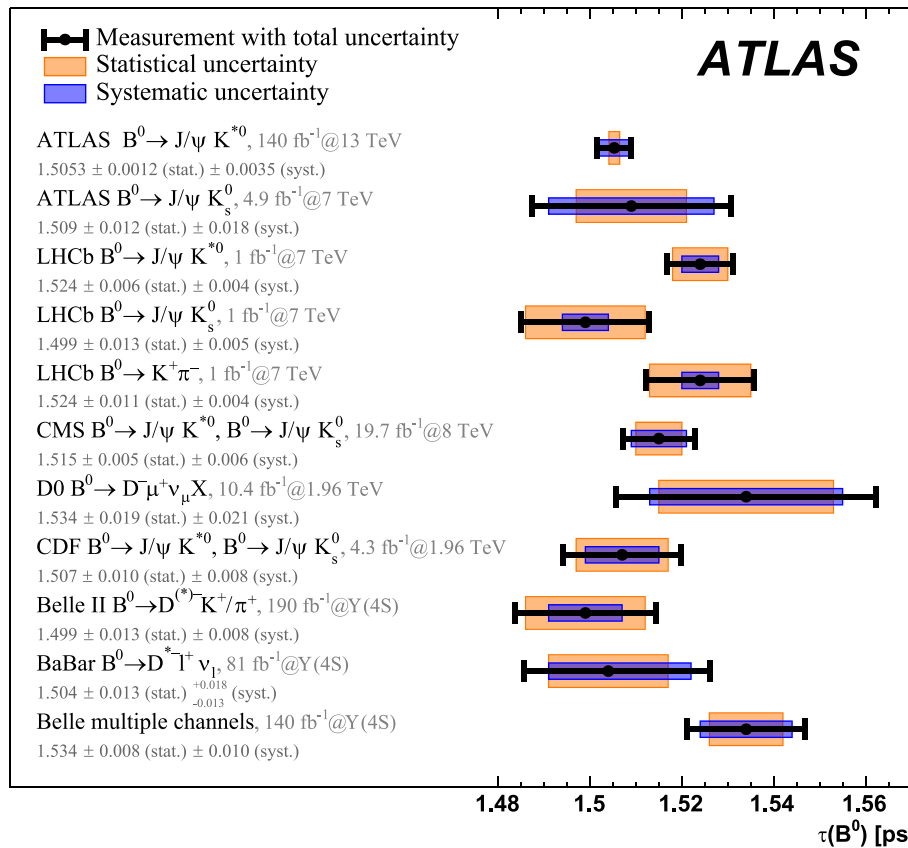


Fig. 3 A comparison of the current ATLAS result for the B^0 lifetime with the previous ATLAS result [18] in the $B^0 \rightarrow J/\psi K_S^0$ channel, and with those from other experiments. For the LHC, there are two measurements by LHCb [19] in $B^0 \rightarrow J/\psi K^{*0}$ and $B^0 \rightarrow J/\psi K_S^0$ decays, another LHCb result [20] in the $B^0 \rightarrow K^+ \pi^-$ channel, and the CMS [21] combined result for $B^0 \rightarrow J/\psi K^{*0}$ and $B^0 \rightarrow J/\psi K_S^0$ decays. Other contributions come from the Tevatron experiments: from D0 [25] in the $B^0 \rightarrow D^* \bar{\ell}^+ \nu_\ell$ channel, and from CDF [24] with a com-

bined result for $B^0 \rightarrow J/\psi K^{*0}$ and $B^0 \rightarrow J/\psi K_S^0$. From $e^+ e^-$ colliders, the leading result from Belle II [22] in the $B^0 \rightarrow D^{*-} K^+ / \pi^+$ channel and the result from BaBar [23] in the $B^0 \rightarrow D^{*-} \ell^+ \nu_\ell$ channel are shown. The last measurement presented is a combination of multiple channels, performed by the Belle experiment [26]. This combination includes measurements from the following decays: $B^0 \rightarrow D^{*-} \ell^+ \nu_\ell$, $B^0 \rightarrow D^{*-} \pi^+$, $B^0 \rightarrow D^- \pi^+$, $B^0 \rightarrow D^{*-} \rho^+$, $B^0 \rightarrow J/\psi K^{*0}$, $B^0 \rightarrow J/\psi K_S^0$

precise modelling of the decays and a decrease in related uncertainties.

The ATLAS Γ_d value extracted from this B^0 lifetime measurement is compatible with the HQE theory prediction of $0.63^{+0.11}_{-0.07} \text{ ps}^{-1}$ [16] within 0.3σ , where the uncertainty σ is estimated by combining the uncertainty of this result and the uncertainty given in Ref. [16]. The ATLAS result for Γ_d / Γ_s is compatible with the theory predictions of HQE and lattice QCD models [16, 17] (see also Table 1) within 1.3σ and 0.4σ , respectively, and with the experimental average (1.001 ± 0.004) [15] within 1.3σ , where the respective σ values are estimated by combining the uncertainties from the ATLAS measurements and the other sources.

8 Conclusions

This paper presents a measurement of the B^0 effective lifetime and the average decay width Γ_d using $B^0 \rightarrow J/\psi K^{*0}$ events reconstructed from a 140 fb^{-1} data sample of pp collisions collected with the ATLAS detector during the $\sqrt{s} = 13 \text{ TeV}$ LHC run. The B^0 effective lifetime is measured to be $\tau_{B^0} = 1.5053 \pm 0.0012 \text{ (stat.)} \pm 0.0035 \text{ (syst.)} \text{ ps}$. This ATLAS result is compatible with other experimental measurements and is the most precise measurement to date. The measured average decay width of the heavy and light B^0 mass eigenstates is $\Gamma_d = 0.6639 \pm 0.0005 \text{ (stat.)} \pm 0.0016 \text{ (syst.)} \pm 0.0038 \text{ (ext.)} \text{ ps}^{-1}$. This value is in good agreement with the theory prediction. The measured average decay width Γ_d is combined with the average decay width Γ_s measured previously by ATLAS to obtain the ratio $\Gamma_d / \Gamma_s = 0.9905 \pm 0.0022 \text{ (stat.)} \pm 0.0036 \text{ (syst.)} \pm 0.0057 \text{ (ext.)}$. This

result is compatible with the theory predictions from HQE and lattice QCD calculations, as well as with the experimental average.

Acknowledgements We thank CERN for the very successful operation of the LHC and its injectors, as well as the support staff at CERN and at our institutions worldwide without whom ATLAS could not be operated efficiently. The crucial computing support from all WLCG partners is acknowledged gratefully, in particular from CERN, the ATLAS Tier-1 facilities at TRIUMF/SFU (Canada), NDGF (Denmark, Norway, Sweden), CC-IN2P3 (France), KIT/GridKA (Germany), INFN-CNAF (Italy), NL-T1 (Netherlands), PIC (Spain), RAL (UK) and BNL (USA), the Tier-2 facilities worldwide and large non-WLCG resource providers. Major contributors of computing resources are listed in Ref. [54]. We gratefully acknowledge the support of ANPCyT, Argentina; YerPhi, Armenia; ARC, Australia; BMWFW and FWF, Austria; ANAS, Azerbaijan; CNPq and FAPESP, Brazil; NSERC, NRC and CFI, Canada; CERN; ANID, Chile; CAS, MOST and NSFC, China; Minciencias, Colombia; MEYS CR, Czech Republic; DNRF and DNSRC, Denmark; IN2P3-CNRS and CEA-DRF/IRFU, France; SRNSFG, Georgia; BMBF, HGF and MPG, Germany; GSRI, Greece; RGC and Hong Kong SAR, China; ISF and Benoziyo Center, Israel; INFN, Italy; MEXT and JSPS, Japan; CNRST, Morocco; NWO, Netherlands; RCN, Norway; MNiSW, Poland; FCT, Portugal; MNE/IFA, Romania; MESTD, Serbia; MSSR, Slovakia; ARIS and MVZI, Slovenia; DSi/NRF, South Africa; MICIU/AEI, Spain; SRC and Wallenberg Foundation, Sweden; SERI, SNSF and Cantons of Bern and Geneva, Switzerland; NSTC, Taipei; TENMAK, Türkiye; STFC/UKRI, United Kingdom; DOE and NSF, United States of America. Individual groups and members have received support from BCKDF, CANARIE, CRC and DRAC, Canada; CERN-CZ, FORTE and PRIMUS, Czech Republic; COST, ERC, ERDF, Horizon 2020, ICSC-NextGenerationEU and Marie Skłodowska-Curie Actions, European Union; Investissements d’Avenir Labex, Investissements d’Avenir Idex and ANR, France; DFG and AvH Foundation, Germany; Herakleitos, Thales and Aristeia programmes co-financed by EU-ESF and the Greek NSRF, Greece; BSF-NSF and MINERVA, Israel; NCN and NAWA, Poland; La Caixa Banking Foundation, CERCA Programme Generalitat de Catalunya and PROMETEO and GenT Programmes Generalitat Valenciana, Spain; Göran Gustafssons Stiftelse, Sweden; The Royal Society and Leverhulme Trust, United Kingdom. In addition, individual members wish to acknowledge support from Armenia: Yerevan Physics Institute (FAPERJ); CERN: European Organization for Nuclear Research (CERN PJAS); Chile: Agencia Nacional de Investigación y Desarrollo (FONDECYT 1230812, FONDECYT 1230987, FONDECYT 1240864); China: Chinese Ministry of Science and Technology (MOST-2023YFA1605700, MOST-2023YFA1609300), for the National Natural Science Foundation of China, harmonise the hyphenation of grant numbers: NSFC-12175119, NSFC-12275265, NSFC-12075060; Czech Republic: Czech Science Foundation (GACR - 24-11373 S), Ministry of Education Youth and Sports (ERC-CZ-LL2327, FORTE CZ.02.01.01/00/22_008/0004632), PRIMUS Research Programme (PRIMUS/21/SCI/017); EU: H2020 European Research Council (ERC - 101002463); European Union: European Research Council (ERC - 948254, ERC 101089007), Horizon 2020 Framework Programme (MUCCA - CHISTERA-19-XAI-00), European Union, Future Artificial Intelligence Research (FAIR-NextGenerationEU PE00000013), Italian Center for High Performance Computing, Big Data and Quantum Computing (ICSC, NextGenerationEU); France: Agence Nationale de la Recherche (ANR-20-CE31-0013, ANR-21-CE31-0013, ANR-21-CE31-0022, ANR-22-EDIR-0002), Investissements d’Avenir Labex (ANR-11-LABX-0012); Germany: Baden-Württemberg Stiftung (BW Stiftung-Postdoc Eliteprogramme), Deutsche Forschungsgemeinschaft (DFG - 469666862, DFG - CR 312/5-2); Italy: Istituto Nazionale di Fisica Nucleare

(ICSC, NextGenerationEU), Ministero dell’Università e della Ricerca (NextGenEU PRIN20223N7F8K M4C2.1.1); Japan: Japan Society for the Promotion of Science (JSPS KAKENHI JP22H01227, JSPS KAKENHI JP22H04944, JSPS KAKENHI JP22KK0227, JSPS KAKENHI JP23KK0245); Netherlands: Netherlands Organisation for Scientific Research (NWO Veni 2020 - VI.Veni.202.179); Norway: Research Council of Norway (RCN-314472); Poland: Ministry of Science and Higher Education (IDUB AGH, POB8, D4 no 9722), Polish National Agency for Academic Exchange (PPN/PPO/2020/1/00002/U/00001), Polish National Science Centre (NCN 2021/42/E/ST2/00350, NCN OPUS nr 2022/47/B/ST2/03059, NCN UMO-2019/34/E/ST2/00393, NCN & H2020 MSCA 945339, UMO-2020/37/B/ST2/01043, UMO-2021/40/C/ST2/00187, UMO-2022/47/O/ST2/00148, UMO-2023/49/B/ST2/04085); Slovenia: Slovenian Research Agency (ARIS grant J1-3010); Spain: Generalitat Valenciana (Artemisa, FEDER, IDIFEDER /2018/048), Ministry of Science and Innovation (MCIN & NextGenEU PCI2022-135018-2, MICIN & FEDER PID2021-125273NB, RYC2019-028510-I, RYC2020-030254-I, RYC2021-031273-I, RYC2022-038164-I), PROMETEO and GenT Programmes Generalitat Valenciana (CIDE-GENT/2019/027); Sweden: Carl Trygger Foundation (CTS 22:2312), Swedish Research Council (VR 2023-04654, VR 2018-00482, VR 2021-03651, VR 2022-03845, VR 2022-04683, VR 2023-03403), Knut and Alice Wallenberg Foundation (KAW 2018.0157, KAW 2018.0458, KAW 2019.0447, KAW 2022.0358); Switzerland: Swiss National Science Foundation (SNSF - PCEFP2_194658); United Kingdom: Leverhulme Trust (Leverhulme Trust RPG-2020-004), Royal Society (NIF-R1-231091); United States of America: U.S. Department of Energy (ECA DE-AC02-76SF00515), Neubauer Family Foundation.

Data Availability Statement This manuscript has no associated data. [Authors’ comment: All ATLAS scientific output is published in journals, and preliminary results are made available in Conference Notes. All are openly available, without restriction on use by external parties beyond copyright law and the standard conditions agreed by CERN. Data associated with journal publications are also made available: tables and data from plots (e.g. cross section values, likelihood profiles, selection efficiencies, cross section limits, ...) are stored in appropriate repositories such as HEPDATA (for this paper, <https://www.hepdata.net/record/ins2849026>). ATLAS also strives to make additional material related to the paper available that allows a reinterpretation of the data in the context of new theoretical models. For example, an extended encapsulation of the analysis is often provided for measurements in the framework of RIVET (<http://rivet.hepforge.org/>).] This information is taken from the ATLAS Data Access Policy, which is a public document that can be downloaded from <http://opendata.cern.ch/record/413>.]

Code Availability Statement This manuscript has no associated code/software. [Authors’ comment: ATLAS collaboration software is open source, and all code necessary to recreate an analysis is publicly available. The Athena (<http://gitlab.cern.ch/atlas/athena>) software repository provides all code needed for calibration and uncertainty application, with configuration files that are also publicly available via Docker containers and cvmfs. The specific code and configurations written in support of this analysis are not public; however, these are internally preserved.]

Open Access This article is licensed under a Creative Commons Attribution 4.0 International License, which permits use, sharing, adaptation, distribution and reproduction in any medium or format, as long as you give appropriate credit to the original author(s) and the source, provide a link to the Creative Commons licence, and indicate if changes were made. The images or other third party material in this article are included in the article’s Creative Commons licence, unless indicated otherwise in a credit line to the material. If material is not included in the article’s Creative Commons licence and your intended use is not permitted by statutory regulation or exceeds the permit-

ted use, you will need to obtain permission directly from the copyright holder. To view a copy of this licence, visit <http://creativecommons.org/licenses/by/4.0/>.

Funded by SCOAP³.

References

- V.A. Khoze, M.A. Shifman, Heavy quarks. *Phys. Usp.* **26**, 387 (1983). <https://doi.org/10.1070/PU1983v02n05ABEH004398>
- M.A. Shifman, M.B. Voloshin, Preasymptotic effects in inclusive weak decays of charmed particles. *Sov. J. Nucl. Phys.* **41**, 120 (1985)
- M.A. Shifman, M.B. Voloshin, Hierarchy of lifetimes of charmed and beautiful hadrons. *Sov. Phys. JETP* **64**, 698 (1986)
- I.I. Bigi, N.G. Uraltsev, Gluonic enhancements in non-spectator beauty decays – an inclusive mirage though an exclusive possibility. *Phys. Lett. B* **280**, 271 (1992). [https://doi.org/10.1016/0370-2693\(92\)90066-D](https://doi.org/10.1016/0370-2693(92)90066-D)
- I.I.Y. Bigi, N.G. Uraltsev, A.I. Vainshtein, Nonperturbative corrections to inclusive beauty and charm decays. QCD versus phenomenological models. *Phys. Lett. B* **293**, 430 (1992). [https://doi.org/10.1016/0370-2693\(92\)90908-M](https://doi.org/10.1016/0370-2693(92)90908-M). [arXiv:hep-ph/9207214](https://arxiv.org/abs/hep-ph/9207214) [Erratum: *Phys. Lett. B* 297 (1992) 477. [https://doi.org/10.1016/0370-2693\(92\)91287-J](https://doi.org/10.1016/0370-2693(92)91287-J)]
- I.I. Bigi, The QCD perspective on lifetimes of heavy-flavour hadrons. (1995). [arXiv:hep-ph/9508408](https://arxiv.org/abs/hep-ph/9508408)
- N. Uraltsev, Heavy quark expansion in beauty and its decays. in *Proc. Int. Sch. Phys. Fermi*, vol. 137, ed. by I.I. Bigi, L. Moroni (1998), p. 329. <https://doi.org/10.3254/978-1-61499-222-6-329>. [arXiv:hep-ph/9804275](https://arxiv.org/abs/hep-ph/9804275)
- M. Neubert, B Decays and the heavy-quark expansion. in *Adv. Ser. Direct. High Energy Phys.*, vol. 15, ed. by A.J. Buras, M. Lindner (1998), p. 239. https://doi.org/10.1142/9789812812667_0003. [arXiv:hep-ph/9702375](https://arxiv.org/abs/hep-ph/9702375)
- A. Lenz, Lifetimes and heavy quark expansion. *Int. J. Mod. Phys. A* **30**, 1543005 (2015). <https://doi.org/10.1142/S0217751X15430058>. [arXiv:1405.3601](https://arxiv.org/abs/1405.3601) [hep-ph]
- M. Kirk, A. Lenz, T. Rauh, Dimension-six matrix elements for meson mixing and lifetimes from sum rules. *JHEP* **12**, 068 (2017). [https://doi.org/10.1007/JHEP12\(2017\)068](https://doi.org/10.1007/JHEP12(2017)068). [arXiv:1711.02100](https://arxiv.org/abs/1711.02100) [hep-ph]. [Erratum: *JHEP* 06 (2020) 162. [https://doi.org/10.1007/JHEP06\(2020\)162](https://doi.org/10.1007/JHEP06(2020)162)]
- M.A. Shifman, A.I. Vainshtein, V.I. Zakharov, QCD and resonance physics. Theoretical foundations. *Nucl. Phys. B* **147**, 385 (1979). [https://doi.org/10.1016/0550-3213\(79\)90022-1](https://doi.org/10.1016/0550-3213(79)90022-1)
- M.A. Shifman, A.I. Vainshtein, V.I. Zakharov, QCD and resonance physics. Applications. *Nucl. Phys. B* **147**, 448 (1979). [https://doi.org/10.1016/0550-3213\(79\)90023-3](https://doi.org/10.1016/0550-3213(79)90023-3)
- H. Georgi, An effective field theory for heavy quarks at low energies. *Phys. Lett. B* **240**, 447 (1990). [https://doi.org/10.1016/0370-2693\(90\)91128-X](https://doi.org/10.1016/0370-2693(90)91128-X)
- R. Fleischer, R. Knechtjens, Effective lifetimes of B_s decays and their constraints on the $B_s^0 - \bar{B}_s^0$ mixing parameters. *Eur. Phys. J. C* **71**, 1789 (2011). <https://doi.org/10.1140/epjc/s10052-011-1789-9>. [arXiv:1109.5115](https://arxiv.org/abs/1109.5115) [hep-ph]
- Heavy Flavour Averaging Group, Averages of b -hadron, c -hadron, and τ -lepton properties as of 2021. *Phys. Rev. D* **107**, 052008 (2023). <https://doi.org/10.1103/PhysRevD.107.052008>. [arXiv:2206.07501](https://arxiv.org/abs/2206.07501) [hep-ex]
- A. Lenz, M.L. Piscopo, A.V. Rusov, Disintegration of beauty: a precision study. *JHEP* **01**, 004 (2023). [https://doi.org/10.1007/JHEP01\(2023\)004](https://doi.org/10.1007/JHEP01(2023)004). [arXiv:2208.02643](https://arxiv.org/abs/2208.02643) [hep-ph]
- D. Becirevic, Theoretical progress in describing the B -meson lifetimes. *PoS HEP* **2001**, 098 (2001). <https://doi.org/10.22323/1.007.0098>
0098. [arXiv:hep-ph/0110124](https://arxiv.org/abs/hep-ph/0110124) <https://doi.org/10.22323/1.007.0098>. [arXiv:hep-ph/0110124](https://arxiv.org/abs/hep-ph/0110124)
- ATLAS Collaboration, Measurement of the Λ_b^0 lifetime and mass in the ATLAS experiment. *Phys. Rev. D* **87**, 032002 (2013). <https://doi.org/10.1103/PhysRevD.87.032002>. [arXiv:1207.2284](https://arxiv.org/abs/1207.2284) [hep-ex]
- LHCb Collaboration, Measurements of the B^+ , B^0 , B_s^0 meson and Λ_b^0 baryon lifetimes. *JHEP* **04**, 114 (2014). [https://doi.org/10.1007/JHEP04\(2014\)114](https://doi.org/10.1007/JHEP04(2014)114). [arXiv:1402.2554](https://arxiv.org/abs/1402.2554) [hep-ex]
- LHCb Collaboration, Effective lifetime measurements in the $B_s^0 \rightarrow K^+ K^-$, $B^0 \rightarrow K^+ \pi^-$ and $B_s^0 \rightarrow \pi^+ K^-$ decays, *Phys. Lett. B* **736**, 446 (2014). <https://doi.org/10.1016/j.physletb.2014.07.051>. [arXiv:1406.7204](https://arxiv.org/abs/1406.7204) [hep-ex]
- CMS Collaboration, Measurement of b hadron lifetimes in pp collisions at $\sqrt{s} = 13$ TeV. *Eur. Phys. J. C* **78**, 457 (2018). <https://doi.org/10.1140/epjc/s10052-018-5929-3>. [arXiv:1710.08949](https://arxiv.org/abs/1710.08949) [hep-ex]
- Belle II Collaboration, Measurement of the B^0 lifetime and flavor-oscillation frequency using hadronic decays reconstructed in 2019–2021 Belle II data. *Phys. Rev. D* **107**, L091102 (2023). <https://doi.org/10.1103/physrevd.107.l091102>. [arXiv:2302.12791](https://arxiv.org/abs/2302.12791) [hep-ex]
- BaBar Collaboration, Measurement of the \bar{B}^0 lifetime and the $B^0 \bar{B}^0$ oscillation frequency using partially reconstructed $\bar{B}^0 \rightarrow D^{*+} \ell^- \bar{\nu}_\ell$ decays. *Phys. Rev. D* **73**, 012004 (2006). <https://doi.org/10.1103/PhysRevD.73.012004>. [arXiv:hep-ex/0507054](https://arxiv.org/abs/hep-ex/0507054)
- CDF Collaboration, Measurement of b hadron lifetimes in exclusive decays containing a J/ψ in $p\bar{p}$ collisions at $\sqrt{s} = 1.96$ TeV. *Phys. Rev. Lett.* **106**, 121804 (2011). <https://doi.org/10.1103/PhysRevLett.106.121804>. [arXiv:1012.3138](https://arxiv.org/abs/1012.3138) [hep-ex]
- D0 Collaboration, Measurement of the B_s^0 lifetime in the flavor-specific decay channel $B_s^0 \rightarrow D_s^- \mu^+ \nu X$. *Phys. Rev. Lett.* **114**, 062001 (2015). <https://doi.org/10.1103/PhysRevLett.114.062001>. [arXiv:1410.1568](https://arxiv.org/abs/1410.1568) [hep-ex]
- B. Collaboration, Improved measurement of CP-violation parameters $\sin 2\phi_1$ and $|\lambda|$, B meson lifetimes, and $B^0 - \bar{B}^0$ mixing parameter Δm_d . *Phys. Rev. D* **71**, 072003 (2005). <https://doi.org/10.1103/PhysRevD.71.072003>. [arXiv:hep-ex/0408111](https://arxiv.org/abs/hep-ex/0408111)
- ATLAS Collaboration, Measurement of the CP -violating phase ϕ_s in $B_s^0 \rightarrow J/\psi \phi$ decays in ATLAS at 13 TeV. *Eur. Phys. J. C* **81**, 342 (2021). <https://doi.org/10.1140/epjc/s10052-021-09011-0>. [arXiv:2001.07115](https://arxiv.org/abs/2001.07115) [hep-ex]
- ATLAS Collaboration, The ATLAS Experiment at the CERN large hadron collider. *JINST* **3**, S08003 (2008). <https://doi.org/10.1088/1748-0221/3/08/S08003>
- ATLAS Collaboration, ATLAS inner tracker pixel detector: technical design report. ATLAS-TDR-030; CERN-LHCC-2017-021 (2017). <https://cds.cern.ch/record/2285585>
- ATLAS Collaboration, ATLAS Insertable B-Layer: technical design report. ATLAS-TDR-19; CERN-LHCC-2010-013 (2010). <https://cds.cern.ch/record/1291633>. Addendum: ATLAS-TDR-19-ADD-1; CERN-LHCC-2012-009 (2012). <https://cds.cern.ch/record/1451888>
- B. Abbott et al., Production and integration of the ATLAS Insertable B-Layer. *JINST* **13**, T05008 (2018). <https://doi.org/10.1088/1748-0221/13/05/T05008>. [arXiv:1803.00844](https://arxiv.org/abs/1803.00844) [physics.ins-det]
- G. Avoni et al., The new LUCID-2 detector for luminosity measurement and monitoring in ATLAS. *JINST* **13**, P07017 (2018). <https://doi.org/10.1088/1748-0221/13/07/P07017>
- ATLAS Collaboration, Performance of the ATLAS trigger system in 2015. *Eur. Phys. J. C* **77**, 317 (2017). <https://doi.org/10.1140/epjc/s10052-017-4852-3>. [arXiv:1611.09661](https://arxiv.org/abs/1611.09661) [hep-ex]
- ATLAS Collaboration, Performance of the ATLAS muon triggers in Run 2. *JINST* **15**, P09015 (2020). <https://doi.org/10.1088/1748-0221/15/09/p09015>. [arXiv:2004.13447](https://arxiv.org/abs/2004.13447) [physics.ins-det]

40. ATLAS Collaboration, ATLAS Pythia 8 tunes to 7 TeV data. ATL-PHYS-PUB-2014-021 (2014). <https://cds.cern.ch/record/1966419>
41. J. Pumplin et al., New generation of parton distributions with uncertainties from global QCD analysis. JHEP **07**, 012 (2002). <https://doi.org/10.1088/1126-6708/2002/07/012>. arXiv:hep-ph/0201195 [hep-ph]
42. ATLAS Collaboration, The ATLAS Simulation Infrastructure. Eur. Phys. J. C **70**, 823 (2010). <https://doi.org/10.1140/epjc/s10052-010-1429-9>. arXiv:1005.4568 [physics.ins-det]
43. S. Agostinelli et al., Geant4 – a simulation toolkit. Nucl. Instrum. Methods A **506**, 250 (2003). [https://doi.org/10.1016/S0168-9002\(03\)01368-8](https://doi.org/10.1016/S0168-9002(03)01368-8)
44. ATLAS Collaboration, Vertex reconstruction performance of the ATLAS detector at $\sqrt{s} = 13$ TeV. ATL-PHYS-PUB-2015-026 (2015). <https://cds.cern.ch/record/2037717>
45. ATLAS Collaboration, Muon reconstruction and identification efficiency in ATLAS using the full Run 2 pp collision data set at $\sqrt{s} = 13$ TeV. Eur. Phys. J. C **81**, 578 (2021). <https://doi.org/10.1140/epjc/s10052-021-09233-2>. arXiv:2012.00578 [hep-ex]
46. Particle Data Group, S. Navas et al., Review of particle physics. Phys. Rev. D **110**, 030001 (2024). <https://doi.org/10.1103/PhysRevD.110.030001>
47. N.L. Johnson, Systems of frequency curves generated by methods of translation. Biometrika **36**, 149 (1949). <https://doi.org/10.1093/biomet/36.1-2.149>
48. G. Punzi, Comments on Likelihood fits with variable resolution (2004). arXiv:physics/0401045 [physics.data-an]
49. M. Pivk, F.R. Le Diberder, sPlot: a statistical tool to unfold data distributions. Nucl. Instrum. Methods A **555**, 356 (2005). <https://doi.org/10.1016/j.nima.2005.08.106>. arXiv:physics/0402083.
50. ATLAS Collaboration, Alignment of the ATLAS inner detector in Run 2. Eur. Phys. J. C **80**, 1194 (2020). <https://doi.org/10.1140/epjc/s10052-020-08700-6>. arXiv:2007.07624 [hep-ex]
51. LHCb Collaboration, Measurement of the polarization amplitudes in $B^0 \rightarrow J/\psi K^*(892)^0$ decays. Phys. Rev. D **88** 052002 (5 2013). <https://doi.org/10.1103/PhysRevD.88.052002>. <https://link.aps.org/doi/10.1103/PhysRevD.88.052002>
52. T. Skwarnicki, A study of the radiative CASCADE transitions between the Upsilon-Prime and Upsilon resonances. PhD thesis: Cracow, INP (1986)
53. S. Jackman, Bayesian analysis for the social sciences (2009). <https://onlinelibrary.wiley.com/doi/book/10.1002/9780470686621>
54. ATLAS Collaboration, ATLAS computing acknowledgements. ATL-SOFT-PUB-2025-001 (2025). <https://cds.cern.ch/record/2922210>

ATLAS Collaboration*

- G. Aad¹⁰⁴, E. Aakvaag¹⁷, B. Abbott¹²³, S. Abdelhameed^{119a}, K. Abeling⁵⁶, N. J. Abicht⁵⁰, S. H. Abidi³⁰, M. Aboelela⁴⁵, A. Aboulhorma^{36e}, H. Abramowicz¹⁵⁵, H. Abreu¹⁵⁴, Y. Abulaiti¹²⁰, B. S. Acharya^{70a,70b,m}, A. Ackermann^{64a}, C. Adam Bourdarios⁴, L. Adamczyk^{87a}, S. V. Addepalli²⁷, M. J. Addison¹⁰³, J. Adelman¹¹⁸, A. Adiguzel^{22c}, T. Adye¹³⁷, A. A. Affolder¹³⁹, Y. Afik⁴⁰, M. N. Agaras¹³, J. Agarwala^{74a,74b}, A. Aggarwal¹⁰², C. Agheorghiesei^{28c}, F. Ahmadov^{39,aa}, W. S. Ahmed¹⁰⁶, S. Ahuja⁹⁷, X. Ai^{63e}, G. Aielli^{77a,77b}, A. Aikot¹⁶⁶, M. Ait Tamlihat^{36e}, B. Aitbenchikh^{36a}, M. Akbıyık¹⁰², T. P. A. Åkesson¹⁰⁰, A. V. Akimov³⁸, D. Akiyama¹⁷¹, N. N. Akolkar²⁵, S. Aktas^{22a}, K. Al Khoury⁴², G. L. Alberghi^{24b}, J. Albert¹⁶⁸, P. Albicocco⁵⁴, G. L. Albouy⁶¹, S. Alderweireldt⁵³, Z. L. Alegria¹²⁴, M. Aleksa³⁷, I. N. Aleksandrov³⁹, C. Alexa^{28b}, T. Alexopoulos¹⁰, F. Alfonsi^{24b}, M. Algren⁵⁷, M. Alhoob¹⁷⁰, B. Ali¹³⁵, H. M. J. Ali⁹³, S. Ali³², S. W. Alibocus⁹⁴, M. Aliev^{34c}, G. Alimonti^{72a}, W. Alkakhi⁵⁶, C. Allaire⁶⁷, B. M. M. Allbrooke¹⁵⁰, J. F. Allen⁵³, C. A. Allendes Flores^{140f}, P. P. Allport²¹, A. Aloisio^{73a,73b}, F. Alonso⁹², C. Alpigiani¹⁴², Z. M. K. Alsolami⁹³, M. Alvarez Estevez¹⁰¹, A. Alvarez Fernandez¹⁰², M. Alves Cardoso⁵⁷, M. G. Alviggi^{73a,73b}, M. Aly¹⁰³, Y. Amaral Coutinho^{84b}, A. Ambler¹⁰⁶, C. Amelung³⁷, M. Ameri¹⁰³, C. G. Ames¹¹¹, D. Amidei¹⁰⁸, B. Amini⁵⁵, K. Amirie¹⁵⁸, S. P. Amor Dos Santos^{133a}, K. R. Amos¹⁶⁶, D. Amperiadou¹⁵⁶, S. An⁸⁵, V. Ananiev¹²⁸, C. Anastopoulos¹⁴³, T. Andeen¹¹, J. K. Anders³⁷, A. C. Anderson⁶⁰, S. Y. Andrean^{48a,48b}, A. Andreazza^{72a,72b}, S. Angelidakis⁹, A. Angerami⁴², A. V. Anisenkov³⁸, A. Annovi^{75a}, C. Antel⁵⁷, E. Antipov¹⁴⁹, M. Antonelli⁵⁴, F. Anulli^{76a}, M. Aoki⁸⁵, T. Aoki¹⁵⁷, M. A. Aparo¹⁵⁰, L. Aperio Bella⁴⁹, C. Appelt¹⁹, A. Apyan²⁷, S. J. Arbiol Val⁸⁸, C. Arcangeletti⁵⁴, A. T. H. Arce⁵², J-F. Arguin¹¹⁰, S. Argyropoulos⁵⁵, J.-H. Arling⁴⁹, O. Arnaez⁴, H. Arnold¹⁴⁹, G. Artoni^{76a,76b}, H. Asada¹¹³, K. Asai¹²¹, S. Asai¹⁵⁷, N. A. Asbah³⁷, R. A. Ashby Pickering¹⁷⁰, K. Assamagan³⁰, R. Astalos^{29a}, K. S. V. Astrand¹⁰⁰, S. Atashi¹⁶², R. J. Atkin^{34a}, M. Atkinson¹⁶⁵, H. Atmani^{36f}, P. A. Atmasiddha¹³¹, K. Augsten¹³⁵, S. Auricchio^{73a,73b}, A. D. Auriol²¹, V. A. Austrup¹⁰³, G. Avolio³⁷, K. Axiotis⁵⁷, G. Azuelos^{110,af}, D. Babal^{29b}, H. Bachacou¹³⁸, K. Bachas^{156,q}, A. Bachiu³⁵, F. Backman^{48a,48b}, A. Badea⁴⁰, T. M. Baer¹⁰⁸, P. Bagnaia^{76a,76b}, M. Bahmani¹⁹, D. Bahner⁵⁵, K. Bai¹²⁶, J. T. Baines¹³⁷, L. Baines⁹⁶, O. K. Baker¹⁷⁵, E. Bakos¹⁶, D. Bakshi Gupta⁸, L. E. Balabram Filho^{84b}, V. Balakrishnan¹²³, R. Balasubramanian¹¹⁷, E. M. Baldin³⁸, P. Balek^{87a}, E. Ballabene^{24b,24a}, F. Balli¹³⁸, L. M. Baltes^{64a}, W. K. Balunas³³, J. Balz¹⁰², I. Bamwidhi^{119b}, E. Banas⁸⁸, M. Bandiermonte¹³², A. Bandyopadhyay²⁵, S. Bansal²⁵, L. Barak¹⁵⁵, M. Barakat⁴⁹, E. L. Barberio¹⁰⁷, D. Barberis^{58a,58b}, M. Barbero¹⁰⁴, M. Z. Barel¹¹⁷, T. Barillari¹¹², M-S. Barisits³⁷

- T. Barklow¹⁴⁷, P. Baron¹²⁵, D. A. Baron Moreno¹⁰³, A. Baroncelli^{63a}, A. J. Barr¹²⁹, J. D. Barr⁹⁸, F. Barreiro¹⁰¹, J. Barreiro Guimarães da Costa¹⁴, U. Barron¹⁵⁵, M. G. Barros Teixeira^{133a}, S. Barsov³⁸, F. Bartels^{64a}, R. Bartoldus¹⁴⁷, A. E. Barton⁹³, P. Bartos^{29a}, A. Basan¹⁰², M. Baselga⁵⁰, A. Bassalat^{67,b}, M. J. Basso^{159a}, S. Bataju⁴⁵, R. Bate¹⁶⁷, R. L. Bates⁶⁰, S. Batlamous¹⁰¹, B. Batool¹⁴⁵, M. Battaglia¹³⁹, D. Battulga¹⁹, M. Bauce^{76a,76b}, M. Bauer⁸⁰, P. Bauer²⁵, L. T. Bazzano Hurrell³¹, J. B. Beacham⁵², T. Beau¹³⁰, J. Y. Beaumamp⁹², P. H. Beauchemin¹⁶¹, P. Bechtle²⁵, H. P. Beck^{20,p}, K. Becker¹⁷⁰, A. J. Beddall⁸³, V. A. Bednyakov³⁹, C. P. Bee¹⁴⁹, L. J. Beemster¹⁶, T. A. Beermann³⁷, M. Begalli^{84d}, M. Begel³⁰, A. Behera¹⁴⁹, J. K. Behr⁴⁹, J. F. Beirer³⁷, F. Beisiegel²⁵, M. Belfkir^{119b}, G. Bella¹⁵⁵, L. Bellagamba^{24b}, A. Bellerive³⁵, P. Bellos²¹, K. Beloborodov³⁸, D. Benchekroun^{36a}, F. Bendebba^{36a}, Y. Benhammou¹⁵⁵, K. C. Benkendorfer⁶², L. Beresford⁴⁹, M. Beretta⁵⁴, E. Bergeaas Kuutmann¹⁶⁴, N. Berger⁴, B. Bergmann¹³⁵, J. Beringer^{18a}, G. Bernardi⁵, C. Bernius¹⁴⁷, F. U. Bernlochner²⁵, F. Bernon^{37,104}, A. Berrocal Guardia¹³, T. Berry⁹⁷, P. Berta¹³⁶, A. Berthold⁵¹, S. Bethke¹¹², A. Betti^{76a,76b}, A. J. Bevan⁹⁶, N. K. Bhalla⁵⁵, S. Bhatta¹⁴⁹, D. S. Bhattacharya¹⁶⁹, P. Bhattacharai¹⁴⁷, K. D. Bhide⁵⁵, V. S. Bhopatkar¹²⁴, R. M. Bianchi¹³², G. Bianco^{24a,24b}, O. Biebel¹¹¹, R. Bielski¹²⁶, M. Biglietti^{78a}, C. S. Billingsley⁴⁵, Y. Bimgni^{36f}, M. Bind⁵⁶, A. Bingul^{22b}, C. Bini^{76a,76b}, G. A. Bird³³, M. Birman¹⁷², M. Biros¹³⁶, S. Biryukov¹⁵⁰, T. Bisanz⁵⁰, E. Bisceglie^{44a,44b}, J. P. Biswal¹³⁷, D. Biswas¹⁴⁵, I. Bloch⁴⁹, A. Blue⁶⁰, U. Blumenschein⁹⁶, J. Blumenthal¹⁰², V. S. Bobrovnikov³⁸, M. Boehler⁵⁵, B. Boehm¹⁶⁹, D. Bogavac³⁷, A. G. Bogdanchikov³⁸, L. S. Boggia¹³⁰, C. Bohm^{48a}, V. Boisvert⁹⁷, P. Bokan³⁷, T. Bold^{87a}, M. Bomben⁵, M. Bona⁹⁶, M. Boonekamp¹³⁸, C. D. Booth⁹⁷, A. G. Borbely⁶⁰, I. S. Bordulev³⁸, G. Borissov⁹³, D. Bortoletto¹²⁹, D. Boscherini^{24b}, M. Bosman¹³, J. D. Bossio Sola³⁷, K. Bouaouda^{36a}, N. Bouchhar¹⁶⁶, L. Boudet⁴, J. Boudreau¹³², E. V. Bouhova-Thacker⁹³, D. Boumediene⁴¹, R. Bouquet^{58a,58b}, A. Boveia¹²², J. Boyd³⁷, D. Boye³⁰, I. R. Boyko³⁹, L. Bozianu⁵⁷, J. Bracinik²¹, N. Brahimi⁴, G. Brandt¹⁷⁴, O. Brandt³³, F. Braren⁴⁹, B. Brau¹⁰⁵, J. E. Brau¹²⁶, R. Brener¹⁷², L. Brenner¹¹⁷, R. Brenner¹⁶⁴, S. Bressler¹⁷², G. Brianti^{79a,79b}, D. Britton⁶⁰, D. Britzger¹¹², I. Brock²⁵, R. Brock¹⁰⁹, G. Brooijmans⁴², E. M. Brooks^{159b}, E. Brost³⁰, L. M. Brown^{168,159a}, L. E. Bruce⁶², T. L. Bruckler¹²⁹, P. A. Bruckman de Renstrom⁸⁸, B. Brüters⁴⁹, A. Bruni^{24b}, G. Bruni^{24b}, M. Bruschi^{24b}, N. Bruscino^{76a,76b}, T. Buanes¹⁷, Q. Buat¹⁴², D. Buchin¹¹², A. G. Buckley⁶⁰, O. Bulekov³⁸, B. A. Bullard¹⁴⁷, S. Burdin⁹⁴, C. D. Burgard⁵⁰, A. M. Burger³⁷, B. Burghgrave⁸, O. Burlayenko⁵⁵, J. Burleson¹⁶⁵, J. T. P. Burr³³, J. C. Burzynski¹⁴⁶, E. L. Busch⁴², V. Büscher¹⁰², P. J. Bussey⁶⁰, J. M. Butler²⁶, C. M. Buttar⁶⁰, J. M. Butterworth⁹⁸, W. Buttinger¹³⁷, C. J. Buxo Vazquez¹⁰⁹, A. R. Buzykaev³⁸, S. Cabrera Urbán¹⁶⁶, L. Cadamuro⁶⁷, D. Caforio⁵⁹, H. Cai¹³², Y. Cai^{14,114c}, Y. Cai^{114a}, V. M. M. Cairo³⁷, O. Cakir^{3a}, N. Calace³⁷, P. Calafiura^{18a}, G. Calderini¹³⁰, P. Calfayan⁶⁹, G. Callea⁶⁰, L. P. Caloba^{84b}, D. Calvet⁴¹, S. Calvet⁴¹, M. Calvetti^{75a,75b}, R. Camacho Toro¹³⁰, S. Camarda³⁷, D. Camarero Munoz²⁷, P. Camarri^{77a,77b}, M. T. Camerlingo^{73a,73b}, D. Cameron³⁷, C. Camincher¹⁶⁸, M. Campanelli⁹⁸, A. Camplani⁴³, V. Canale^{73a,73b}, A. C. Canbay^{3a}, E. Canonero⁹⁷, J. Cantero¹⁶⁶, Y. Cao¹⁶⁵, F. Capocasa²⁷, M. Capua^{44a,44b}, A. Carbone^{72a,72b}, R. Cardarelli^{77a}, J. C. J. Cardenas⁸, G. Carducci^{44a,44b}, T. Carli³⁷, G. Carlino^{73a}, J. I. Carlotto¹³, B. T. Carlson^{132,r}, E. M. Carlson^{168,159a}, J. Carmignani⁹⁴, L. Carminati^{72a,72b}, A. Carnelli¹³⁸, M. Carnesale^{76a,76b}, S. Caron¹¹⁶, E. Carquin^{140f}, S. Carrá^{72a}, G. Carratta^{24a,24b}, A. M. Carroll¹²⁶, T. M. Carter⁵³, M. P. Casado^{13,j}, M. Caspar⁴⁹, F. L. Castillo⁴, L. Castillo Garcia¹³, V. Castillo Gimenez¹⁶⁶, N. F. Castro^{133a,133e}, A. Catinaccio³⁷, J. R. Catmore¹²⁸, T. Cavalieri⁴, V. Cavalieri³⁰, N. Cavalli^{24a,24b}, L. J. Caviedes Betancourt^{23b}, Y. C. Cekmecelioglu⁴⁹, E. Celebi⁸³, S. Cella³⁷, F. Celli¹²⁹, M. S. Centonze^{71a,71b}, V. Cepaitis⁵⁷, K. Cerny¹²⁵, A. S. Cerqueira^{84a}, A. Cerri¹⁵⁰, L. Cerrito^{77a,77b}, F. Cerutti^{18a}, B. Cervato¹⁴⁵, A. Cervelli^{24b}, G. Cesarin⁵⁴, S. A. Cetin⁸³, D. Chakraborty¹¹⁸, J. Chan^{18a}, W. Y. Chan¹⁵⁷, J. D. Chapman³³, E. Chapon¹³⁸, B. Chargeishvili^{153b}, D. G. Charlton²¹, M. Chatterjee²⁰, C. Chauhan¹³⁶, Y. Che^{114a}, S. Chekanov⁶, S. V. Chekulaev^{159a}, G. A. Chelkov^{39,a}, A. Chen¹⁰⁸, B. Chen¹⁵⁵, B. Chen¹⁶⁸, H. Chen^{114a}, H. Chen³⁰, J. Chen^{63c}, J. Chen¹⁴⁶, M. Chen¹²⁹, S. Chen¹⁵⁷, S. J. Chen^{114a}, X. Chen^{63c}, X. Chen^{15,ae}, Y. Chen^{63a}, C. L. Cheng¹⁷³, H. C. Cheng^{65a}, S. Cheong¹⁴⁷, A. Cheplakov³⁹, E. Cheremushkina⁴⁹, E. Cherepanova¹¹⁷, R. Cherkaoui El Moursli^{36e}, E. Cheu⁷, K. Cheung⁶⁶, L. Chevalier¹³⁸, V. Chiarella⁵⁴, G. Chiarelli^{75a}, N. Chiedde¹⁰⁴, G. Chiodini^{71a}, A. S. Chisholm²¹, A. Chitan^{28b}, M. Chitishvili¹⁶⁶, M. V. Chizhov^{39,s}, K. Choi¹¹, Y. Chou¹⁴², E. Y. S. Chow¹¹⁶, K. L. Chu¹⁷², M. C. Chu^{65a}, X. Chu^{14,114c}, Z. Chubinidze⁵⁴, J. Chudoba¹³⁴, J. J. Chwastowski⁸⁸, D. Cieri¹¹², K. M. Ciesla^{87a}, V. Cindro⁹⁵, A. Ciocio^{18a}, F. Cirotto^{73a,73b}, Z. H. Citron¹⁷², M. Citterio^{72a}, D. A. Ciubotaru^{28b}, A. Clark⁵⁷, P. J. Clark⁵³

- N. Clarke Hall⁹⁸, C. Clarry¹⁵⁸, J. M. Clavijo Columbie⁴⁹, S. E. Clawson⁴⁹, C. Clement^{48a,48b}, Y. Coadou¹⁰⁴, M. Cobal^{70a,70c}, A. Coccaro^{58b}, R. F. Coelho Barrue^{133a}, R. Coelho Lopes De Sa¹⁰⁵, S. Coelli^{72a}, B. Cole⁴², J. Collot⁶¹, P. Conde Muiño^{133a,133g}, M. P. Connell^{34c}, S. H. Connell^{34c}, E. I. Conroy¹²⁹, F. Conventi^{73a,ag}, H. G. Cooke²¹, A. M. Cooper-Sarkar¹²⁹, F. A. Corchia^{24a,24b}, A. Cordeiro Oudot Choi¹³⁰, L. D. Corpe⁴¹, M. Corradi^{76a,76b}, F. Corriveau^{106,y}, A. Cortes-Gonzalez¹⁹, M. J. Costa¹⁶⁶, F. Costanza⁴, D. Costanzo¹⁴³, B. M. Cote¹²², J. Couthures⁴, G. Cowan⁹⁷, K. Cranmer¹⁷³, D. Cremonini^{24a,24b}, S. Crépé-Renaudin⁶¹, F. Crescioli¹³⁰, M. Cristinziani¹⁴⁵, M. Cristoforetti^{79a,79b}, V. Croft¹¹⁷, J. E. Crosby¹²⁴, G. Crosetti^{44a,44b}, A. Cueto¹⁰¹, H. Cui⁹⁸, Z. Cui⁷, W. R. Cunningham⁶⁰, F. Curcio¹⁶⁶, J. R. Curran⁵³, P. Czodrowski³⁷, M. J. Da Cunha Sargedas De Sousa^{58a,58b}, J. V. Da Fonseca Pinto^{84b}, C. Da Via¹⁰³, W. Dabrowski^{87a}, T. Dado³⁷, S. Dahbi¹⁵², T. Dai¹⁰⁸, D. Dal Santo²⁰, C. Dallapiccola¹⁰⁵, M. Dam⁴³, G. D'amen³⁰, V. D'Amico¹¹¹, J. Damp¹⁰², J. R. Dandoy³⁵, D. Dannheim³⁷, M. Danninger¹⁴⁶, V. Dao¹⁴⁹, G. Darbo^{58b}, S. J. Das^{30,ah}, F. Dattola⁴⁹, S. D'Auria^{72a,72b}, A. D'Avanzo^{73a,73b}, C. David^{34a}, T. Davidek¹³⁶, I. Dawson⁹⁶, H. A. Day-hall¹³⁵, K. De⁸, R. De Asmundis^{73a}, N. De Biase⁴⁹, S. De Castro^{24a,24b}, N. De Groot¹¹⁶, P. de Jong¹¹⁷, H. De la Torre¹¹⁸, A. De Maria^{114a}, A. De Salvo^{76a}, U. De Sanctis^{77a,77b}, F. De Santis^{71a,71b}, A. De Santo¹⁵⁰, J. B. De Vivie De Regie⁶¹, J. Debenc⁹⁵, D. V. Dedovich³⁹, J. Degens⁹⁴, A. M. Deiana⁴⁵, F. Del Corso^{24a,24b}, J. Del Peso¹⁰¹, L. Delagrange¹³⁰, F. Deliot¹³⁸, C. M. Delitzsch⁵⁰, M. Della Pietra^{73a,73b}, D. Della Volpe⁵⁷, A. Dell'Acqua³⁷, L. Dell'Asta^{72a,72b}, M. Delmastro⁴, P. A. Delsart⁶¹, S. Demers¹⁷⁵, M. Demichev³⁹, S. P. Denisov³⁸, L. D'Eramo⁴¹, D. Derendarz⁸⁸, F. Derue¹³⁰, P. Dervan⁹⁴, K. Desch²⁵, C. Deutsch²⁵, F. A. Di Bello^{58a,58b}, A. Di Ciaccio^{77a,77b}, L. Di Ciaccio⁴, A. Di Domenico^{76a,76b}, C. Di Donato^{73a,73b}, A. Di Girolamo³⁷, G. Di Gregorio³⁷, A. Di Luca^{79a,79b}, B. Di Micco^{78a,78b}, R. Di Nardo^{78a,78b}, K. F. Di Petrillo⁴⁰, M. Diamantopoulou³⁵, F. A. Dias¹¹⁷, T. Dias Do Vale¹⁴⁶, M. A. Diaz^{140a,140b}, F. G. Diaz Capriles²⁵, A. R. Didenko³⁹, M. Didenko¹⁶⁶, E. B. Diehl¹⁰⁸, S. Díez Cornell⁴⁹, C. Diez Pardos¹⁴⁵, C. Dimitriadi¹⁶⁴, A. Dimitrieva²¹, J. Dingfelder²⁵, T. Dingley¹²⁹, I-M. Dinu^{28b}, S. J. Dittmeier^{64b}, F. Dittus³⁷, M. Divisek¹³⁶, B. Dixit⁹⁴, F. Djama¹⁰⁴, T. Djobava^{153b}, C. Doglioni^{100,103}, A. Dohnalova^{29a}, J. Dolejsi¹³⁶, Z. Dolezal¹³⁶, K. Domijan^{87a}, K. M. Dona⁴⁰, M. Donadelli^{84d}, B. Dong¹⁰⁹, J. Donini⁴¹, A. D'Onofrio^{73a,73b}, M. D'Onofrio⁹⁴, J. Dopke¹³⁷, A. Doria^{73a}, N. Dos Santos Fernandes^{133a}, P. Dougan¹⁰³, M. T. Dova⁹², A. T. Doyle⁶⁰, M. A. Draguet¹²⁹, E. Dreyer¹⁷², I. Drivas-koulouris¹⁰, M. Drnevich¹²⁰, M. Drozdova⁵⁷, D. Du^{63a}, T. A. du Pree¹¹⁷, F. Dubinin³⁸, M. Dubovsky^{29a}, E. Duchovni¹⁷², G. Duckeck¹¹¹, O. A. Ducu^{28b}, D. Duda⁵³, A. Dudarev³⁷, E. R. Duden²⁷, M. D'uffizi¹⁰³, L. Duflot⁶⁷, M. Dührssen³⁷, I. Duminica^{28g}, A. E. Dumitriu^{28b}, M. Dunford^{64a}, S. Dungs⁵⁰, K. Dunne^{48a,48b}, A. Duperrin¹⁰⁴, H. Duran Yildiz^{3a}, M. Düren⁵⁹, A. Durglishvili^{153b}, B. L. Dwyer¹¹⁸, G. I. Dyckes^{18a}, M. Dyndal^{87a}, B. S. Dziedzic³⁷, Z. O. Earnshaw¹⁵⁰, G. H. Eberwein¹²⁹, B. Eckerova^{29a}, S. Eggebrecht⁵⁶, E. Egidio Purcino De Souza^{84e}, L. F. Ehrke⁵⁷, G. Eigen¹⁷, K. Einsweiler^{18a}, T. Ekelof¹⁶⁴, P. A. Ekman¹⁰⁰, S. El Farkh^{36b}, Y. El Ghazali^{63a}, H. El Jarrari³⁷, A. El Moussaoui^{36a}, V. Ellajosyula¹⁶⁴, M. Ellert¹⁶⁴, F. Ellinghaus¹⁷⁴, N. Ellis³⁷, J. Elmsheuser³⁰, M. Elsawy^{119a}, M. Elsing³⁷, D. Emeliyanov¹³⁷, Y. Enari⁸⁵, I. Ene^{18a}, S. Epari¹³, P. A. Erland⁸⁸, D. Ernani Martins Neto⁸⁸, M. Errenst¹⁷⁴, M. Escalier⁶⁷, C. Escobar¹⁶⁶, E. Etzion¹⁵⁵, G. Evans^{133a,133b}, H. Evans⁶⁹, L. S. Evans⁹⁷, A. Ezhilov³⁸, S. Ezzarqtouni^{36a}, F. Fabbri^{24a,24b}, L. Fabbri^{24a,24b}, G. Facini⁹⁸, V. Fadeyev¹³⁹, R. M. Fakhrutdinov³⁸, D. Fakoudis¹⁰², S. Falciano^{76a}, L. F. Falda Ulhoa Coelho³⁷, F. Fallavollita¹¹², G. Falsetti^{44a,44b}, J. Faltova¹³⁶, C. Fan¹⁶⁵, K. Y. Fan^{65b}, Y. Fan¹⁴, Y. Fang^{14,114c}, M. Fanti^{72a,72b}, M. Faraj^{70a,70b}, Z. Farazpay⁹⁹, A. Farbin⁸, A. Farilla^{78a}, T. Farooque¹⁰⁹, S. M. Farrington⁵³, F. Fassi^{36e}, D. Fassouliotis⁹, M. Faucci Giannelli^{77a,77b}, W. J. Fawcett³³, L. Fayard⁶⁷, P. Federic¹³⁶, P. Federicova¹³⁴, O. L. Fedin^{38.a}, M. Feickert¹⁷³, L. Feligioni¹⁰⁴, D. E. Fellers¹²⁶, C. Feng^{63b}, Z. Feng¹¹⁷, M. J. Fenton¹⁶², L. Ferencz⁴⁹, R. A. M. Ferguson⁹³, S. I. Fernandez Luengo^{140f}, P. Fernandez Martinez⁶⁸, M. J. V. Fernoux¹⁰⁴, J. Ferrando⁹³, A. Ferrari¹⁶⁴, P. Ferrari^{116,117}, R. Ferrari^{74a}, D. Ferrere⁵⁷, C. Ferretti¹⁰⁸, D. Fiacco^{76a,76b}, F. Fiedler¹⁰², P. Fiedler¹³⁵, A. Filipčič⁹⁵, E. K. Filmer¹, F. Filthaut¹¹⁶, M. C. N. Fiolhais^{133a,133c,c}, L. Fiorini¹⁶⁶, W. C. Fisher¹⁰⁹, T. Fitschen¹⁰³, P. M. Fitzhugh¹³⁸, I. Fleck¹⁴⁵, P. Fleischmann¹⁰⁸, T. Flick¹⁷⁴, M. Flores^{34d,ac}, L. R. Flores Castillo^{65a}, L. Flores Sanz De Acedo³⁷, F. M. Follega^{79a,79b}, N. Fomin³³, J. H. Foo¹⁵⁸, A. Formica¹³⁸, A. C. Forti¹⁰³, E. Fortin³⁷, A. W. Fortman^{18a}, M. G. Foti^{18a}, L. Fountas^{9,k}, D. Fournier⁶⁷, H. Fox⁹³, P. Francavilla^{75a,75b}, S. Francescato⁶², S. Franchellucci⁵⁷, M. Franchini^{24a,24b}, S. Franchino^{64a}, D. Francis³⁷, L. Franco¹¹⁶, V. Franco Lima³⁷, L. Franconi⁴⁹, M. Franklin⁶², G. Frattari²⁷, Y. Y. Frid¹⁵⁵, J. Friend⁶⁰, N. Fritzsche³⁷, A. Froch⁵⁵, D. Froidevaux³⁷, J. A. Frost¹²⁹, Y. Fu^{63a}, S. Fuenzalida Garrido^{140f}, M. Fujimoto¹⁰⁴, K. Y. Fung^{65a}, E. Furtado De Simas Filho^{84e}, M. Furukawa¹⁵⁷, J. Fuster¹⁶⁶, A. Gaa⁵⁶

- A. Gabrielli^{24a,24b}, A. Gabrielli¹⁵⁸, P. Gadow³⁷, G. Gagliardi^{58a,58b}, L. G. Gagnon^{18a}, S. Gaid¹⁶³, S. Galantzan¹⁵⁵, J. Gallagher¹, E. J. Gallas¹²⁹, B. J. Gallop¹³⁷, K. K. Gan¹²², S. Ganguly¹⁵⁷, Y. Gao⁵³, F. M. Garay Walls^{140a,140b}, B. Garcia³⁰, C. Garcia¹⁶⁶, A. Garcia Alonso¹¹⁷, A. G. Garcia Caffaro¹⁷⁵, J. E. Garcia Navarro¹⁶⁶, M. Garcia-Siveres^{18a}, G. L. Gardner¹³¹, R. W. Gardner⁴⁰, N. Garelli¹⁶¹, D. Garg⁸¹, R. B. Garg¹⁴⁷, J. M. Gargan⁵³, C. A. Garner¹⁵⁸, C. M. Garvey^{34a}, V. K. Gassmann¹⁶¹, G. Gaudio^{74a}, V. Gautam¹³, P. Gauzzi^{76a,76b}, J. Gavranovic⁹⁵, I. L. Gavrilenko³⁸, A. Gavrilyuk³⁸, C. Gay¹⁶⁷, G. Gaycken¹²⁶, E. N. Gazis¹⁰, A. A. Geanta^{28b}, C. M. Gee¹³⁹, A. Gekow¹²², C. Gemme^{58b}, M. H. Genest⁶¹, A. D. Gentry¹¹⁵, S. George⁹⁷, W. F. George²¹, T. Geralis⁴⁷, P. Gessinger-Befurt³⁷, M. E. Geyik¹⁷⁴, M. Ghani¹⁷⁰, K. Ghorbanian⁹⁶, A. Ghosal¹⁴⁵, A. Ghosh¹⁶², B. Giacobbe^{24b}, S. Giagu^{76a,76b}, T. Giani¹¹⁷, A. Giannini^{63a}, S. M. Gibson⁹⁷, M. Gignac¹³⁹, D. T. Gil^{87b}, A. K. Gilbert^{87a}, B. J. Gilbert⁴², D. Gillberg³⁵, G. Gilles¹¹⁷, L. Ginabat¹³⁰, D. M. Gingrich^{2,af}, M. P. Giordani^{70a,70c}, P. F. Giraud¹³⁸, G. Giugliarelli^{70a,70c}, D. Giugni^{72a}, F. Giuli³⁷, I. Gkialas^{9,k}, L. K. Gladilin³⁸, C. Glasman¹⁰¹, G. R. Gledhill¹²⁶, G. Glemža⁴⁹, M. Glisic¹²⁶, I. Gnesi^{44b,f}, Y. Go³⁰, M. Goblirsch-Kolb³⁷, B. Gocke⁵⁰, D. Godin¹¹⁰, B. Gokturk^{22a}, S. Goldfarb¹⁰⁷, T. Golling⁵⁷, M. G. D. Gololo^{34g}, D. Golubkov³⁸, J. P. Gombas¹⁰⁹, A. Gomes^{133a,133b}, G. Gomes Da Silva¹⁴⁵, A. J. Gomez Delegido¹⁶⁶, R. Gonçalo^{133a}, L. Gonella²¹, A. Gongadze^{153c}, F. Gonnella²¹, J. L. Gonski¹⁴⁷, R. Y. González Andana⁵³, S. González de la Hoz¹⁶⁶, R. Gonzalez Lopez⁹⁴, C. Gonzalez Renteria^{18a}, M. V. Gonzalez Rodrigues⁴⁹, R. Gonzalez Suarez¹⁶⁴, S. Gonzalez-Sevilla⁵⁷, L. Goossens³⁷, B. Gorini³⁷, E. Gorini^{71a,71b}, A. Gorišek⁹⁵, T. C. Gosart¹³¹, A. T. Goshaw⁵², M. I. Gostkin³⁹, S. Goswami¹²⁴, C. A. Gottardo³⁷, S. A. Gotz¹¹¹, M. Gouighri^{36b}, V. Goumarre⁴⁹, A. G. Goussiou¹⁴², N. Govender^{34c}, R. P. Grabarczyk¹²⁹, I. Grabowska-Bold^{87a}, K. Graham³⁵, E. Gramstad¹²⁸, S. Grancagnolo^{71a,71b}, C. M. Grant^{1,138}, P. M. Gravila^{28f}, F. G. Gravili^{71a,71b}, H. M. Gray^{18a}, M. Greco^{71a,71b}, M. J. Green¹, C. Grefe²⁵, A. S. Grefsrud¹⁷, I. M. Gregor⁴⁹, K. T. Greif¹⁶², P. Grenier¹⁴⁷, S. G. Grewe¹¹², A. A. Grillo¹³⁹, K. Grimm³², S. Grinstein^{13,u}, J.-F. Grivaz⁶⁷, E. Gross¹⁷², J. Grosse-Knetter⁵⁶, L. Guan¹⁰⁸, J. G. R. Guerrero Rojas¹⁶⁶, G. Guerrieri³⁷, R. Gugel¹⁰², J. A. M. Guhit¹⁰⁸, A. Guida¹⁹, E. Guilloton¹⁷⁰, S. Guindon³⁷, F. Guo^{14,114c}, J. Guo^{63c}, L. Guo⁴⁹, Y. Guo¹⁰⁸, R. Gupta¹³², S. Gurbuz²⁵, S. S. Gurdasani⁵⁵, G. Gustavino^{76a,76b}, P. Gutierrez¹²³, L. F. Gutierrez Zagazeta¹³¹, M. Gutsche⁵¹, C. Gutschow⁹⁸, C. Gwenlan¹²⁹, C. B. Gwilliam⁹⁴, E. S. Haaland¹²⁸, A. Haas¹²⁰, M. Habedank⁴⁹, C. Haber^{18a}, H. K. Hadavand⁸, A. Hadef⁵¹, S. Hadzic¹¹², A. I. Hagan⁹³, J. J. Hahn¹⁴⁵, E. H. Haines⁹⁸, M. Haleem¹⁶⁹, J. Haley¹²⁴, J. J. Hall¹⁴³, G. D. Hallewell¹⁰⁴, L. Halser²⁰, K. Hamano¹⁶⁸, M. Hamer²⁵, G. N. Hamity⁵³, E. J. Hampshire⁹⁷, J. Han^{63b}, K. Han^{63a}, L. Han^{114a}, L. Han^{63a}, S. Han^{18a}, Y. F. Han¹⁵⁸, K. Hanagaki⁸⁵, M. Hance¹³⁹, D. A. Hangal⁴², H. Hanif¹⁴⁶, M. D. Hank¹³¹, J. B. Hansen⁴³, P. H. Hansen⁴³, D. Harada⁵⁷, T. Harenberg¹⁷⁴, S. Harkusha³⁸, M. L. Harris¹⁰⁵, Y. T. Harris²⁵, J. Harrison¹³, N. M. Harrison¹²², P. F. Harrison¹⁷⁰, N. M. Hartman¹¹², N. M. Hartmann¹¹¹, R. Z. Hasan^{97,137}, Y. Hasegawa¹⁴⁴, F. Haslbeck¹²⁹, S. Hassan¹⁷, R. Hauser¹⁰⁹, C. M. Hawkes²¹, R. J. Hawkings³⁷, Y. Hayashi¹⁵⁷, D. Hayden¹⁰⁹, C. Hayes¹⁰⁸, R. L. Hayes¹¹⁷, C. P. Hays¹²⁹, J. M. Hays⁹⁶, H. S. Hayward⁹⁴, F. He^{63a}, M. He^{14,114c}, Y. He⁴⁹, Y. He⁹⁸, N. B. Heatley⁹⁶, V. Hedberg¹⁰⁰, A. L. Heggelund¹²⁸, N. D. Hehir^{96,*}, C. Heidegger⁵⁵, K. K. Heidegger⁵⁵, J. Heilman³⁵, S. Heim⁴⁹, T. Heim^{18a}, J. G. Heinlein¹³¹, J. J. Heinrich¹²⁶, L. Heinrich^{112,ad}, J. Hejbal¹³⁴, A. Held¹⁷³, S. Hellesund¹⁷, C. M. Helling¹⁶⁷, S. Hellman^{48a,48b}, R. C. W. Henderson⁹³, L. Henkelmann³³, A. M. Henrique Correia³⁷, H. Herde¹⁰⁰, Y. Hernández Jiménez¹⁴⁹, L. M. Herrmann²⁵, T. Herrmann⁵¹, G. Herten⁵⁵, R. Hertenberger¹¹¹, L. Hervas³⁷, M. E. Hesping¹⁰², N. P. Hessey^{159a}, M. Hidaoui^{36b}, N. Hidic¹³⁶, E. Hill¹⁵⁸, S. J. Hillier²¹, J. R. Hinds¹⁰⁹, F. Hinterkeuser²⁵, M. Hirose¹²⁷, S. Hirose¹⁶⁰, D. Hirschbuehl¹⁷⁴, T. G. Hitchings¹⁰³, B. Hiti⁹⁵, J. Hobbs¹⁴⁹, R. Hobincu^{28e}, N. Hod¹⁷², M. C. Hodgkinson¹⁴³, B. H. Hodkinson¹²⁹, A. Hoecker³⁷, D. D. Hofer¹⁰⁸, J. Hofer⁴⁹, T. Holm²⁵, M. Holzbock³⁷, L. B. A. H. Hommels³³, B. P. Honan¹⁰³, J. J. Hong⁶⁹, J. Hong^{63c}, T. M. Hong¹³², B. H. Hooberman¹⁶⁵, W. H. Hopkins⁶, M. C. Hoppesch¹⁶⁵, Y. Horii¹¹³, M. E. Horstmann¹¹², S. Hou¹⁵², A. S. Howard⁹⁵, J. Howarth⁶⁰, J. Hoya⁶, M. Hrabovsky¹²⁵, A. Hrynevich⁴⁹, T. Hrynev'ova⁴, P. J. Hsu⁶⁶, S.-C. Hsu¹⁴², T. Hsu⁶⁷, M. Hu^{18a}, Q. Hu^{63a}, S. Huang^{65b}, X. Huang^{14,114c}, Y. Huang¹⁴³, Y. Huang¹⁰², Y. Huang¹⁴, Z. Huang¹⁰³, Z. Hubacek¹³⁵, M. Huebner²⁵, F. Huegging²⁵, T. B. Huffman¹²⁹, C. A. Hugli⁴⁹, M. Huhtinen³⁷, S. K. Huiberts¹⁷, R. Hulskens¹⁰⁶, N. Huseynov^{12,h}, J. Huston¹⁰⁹, J. Huth⁶², R. Hyneman¹⁴⁷, G. Iacobucci⁵⁷, G. Iakovidis³⁰, L. Iconomidou-Fayard⁶⁷, J. P. Iddon³⁷, P. Iengo^{73a,73b}, R. Iguchi¹⁵⁷, Y. Iiyama¹⁵⁷, T. Iizawa¹²⁹, Y. Ikegami⁸⁵, N. Ilic¹⁵⁸, H. Imam^{84c}, G. Inacio Goncalves^{84d}, M. Ince Lezki⁵⁷, T. Ingebretsen Carlson^{48a,48b}, J. M. Inglis⁹⁶, G. Introzzi^{74a,74b}, M. Iodice^{78a}, V. Ippolito^{76a,76b}, R. K. Irwin⁹⁴, M. Ishino¹⁵⁷, W. Islam¹⁷³, C. Issever^{19,49}, S. Istin^{22a,aj}, H. Ito¹⁷¹, R. Iuppa^{79a,79b}

- A. Ivina¹⁷², J. M. Izen⁴⁶, V. Izzo^{73a}, P. Jacka¹³⁴, P. Jackson¹, C. S. Jagfeld¹¹¹, G. Jain^{159a}, P. Jain⁴⁹, K. Jakobs⁵⁵, T. Jakoubek¹⁷², J. Jamieson⁶⁰, W. Jang¹⁵⁷, M. Javurkova¹⁰⁵, P. Jawahar¹⁰³, L. Jeanty¹²⁶, J. Jejelava^{153a,ab}, P. Jenni^{55,g}, C. E. Jessiman³⁵, C. Jia^{63b}, J. Jia¹⁴⁹, X. Jia^{14,114c}, Z. Jia^{114a}, C. Jiang⁵³, S. Jiggins⁴⁹, J. Jimenez Pena¹³, S. Jin^{114a}, A. Jinaru^{28b}, O. Jinnouchi¹⁴¹, P. Johansson¹⁴³, K. A. Johns⁷, J. W. Johnson¹³⁹, F. A. Jolly⁴⁹, D. M. Jones¹⁵⁰, E. Jones⁴⁹, K. S. Jones⁸, P. Jones³³, R. W. L. Jones⁹³, T. J. Jones⁹⁴, H. L. Joos^{37,56}, R. Joshi¹²², J. Jovicevic¹⁶, X. Ju^{18a}, J. J. Junggeburth¹⁰⁵, T. Junkermann^{64a}, A. Juste Rozas^{13,u}, M. K. Juzek⁸⁸, S. Kabana^{140e}, A. Kaczmarska⁸⁸, M. Kado¹¹², H. Kagan¹²², M. Kagan¹⁴⁷, A. Kahn¹³¹, C. Kahra¹⁰², T. Kaji¹⁵⁷, E. Kajomovitz¹⁵⁴, N. Kakati¹⁷², I. Kalaitzidou⁵⁵, C. W. Kalderon³⁰, N. J. Kang¹³⁹, D. Kar^{34g}, K. Karava¹²⁹, M. J. Kareem^{159b}, E. Karentzos⁵⁵, O. Karkout¹¹⁷, S. N. Karpov³⁹, Z. M. Karpova³⁹, V. Kartvelishvili⁹³, A. N. Karyukhin³⁸, E. Kasimi¹⁵⁶, J. Katzy⁴⁹, S. Kaur³⁵, K. Kawade¹⁴⁴, M. P. Kawale¹²³, C. Kawamoto⁸⁹, T. Kawamoto^{63a}, E. F. Kay³⁷, F. I. Kaya¹⁶¹, S. Kazakos¹⁰⁹, V. F. Kazanin³⁸, Y. Ke¹⁴⁹, J. M. Keaveney^{34a}, R. Keeler¹⁶⁸, G. V. Kehris⁶², J. S. Keller³⁵, A. S. Kelly⁹⁸, J. J. Kempster¹⁵⁰, P. D. Kennedy¹⁰², O. Kepka¹³⁴, B. P. Kerridge¹³⁷, S. Kersten¹⁷⁴, B. P. Kerševan⁹⁵, L. Keszeghova^{29a}, S. Ketabchi Haghigat¹⁵⁸, R. A. Khan¹³², A. Khanov¹²⁴, A. G. Kharlamov³⁸, T. Kharlamova³⁸, E. E. Khoda¹⁴², M. Kholodenko^{133a}, T. J. Khoo¹⁹, G. Khoriauli¹⁶⁹, J. Khubua^{153b,*}, Y. A. R. Khwaira¹³⁰, B. Kibirige^{34g}, D. Kim⁶, D. W. Kim^{48a,48b}, Y. K. Kim⁴⁰, N. Kimura⁹⁸, M. K. Kingston⁵⁶, A. Kirchhoff⁵⁶, C. Kirfel²⁵, F. Kirfel²⁵, J. Kirk¹³⁷, A. E. Kiryunin¹¹², S. Kita¹⁶⁰, C. Kitsaki¹⁰, O. Kivernyk²⁵, M. Klassen¹⁶¹, C. Klein³⁵, L. Klein¹⁶⁹, M. H. Klein⁴⁵, S. B. Klein⁵⁷, U. Klein⁹⁴, P. Klimek³⁷, A. Klimentov³⁰, T. Klioutchnikova³⁷, P. Kluit¹¹⁷, S. Kluth¹¹², E. Kneringer⁸⁰, T. M. Knight¹⁵⁸, A. Knue⁵⁰, M. Kobel⁵¹, D. Kobylanski¹⁷², S. F. Koch¹²⁹, M. Kocian¹⁴⁷, P. Kodyš¹³⁶, D. M. Koeck¹²⁶, P. T. Koenig²⁵, T. Koffas³⁵, O. Kolay⁵¹, I. Koletsou⁴, T. Komarek⁸⁸, K. Köneke⁵⁵, A. X. Y. Kong¹, T. Kono¹²¹, N. Konstantinidis⁹⁸, P. Kontaxakis⁵⁷, B. Konya¹⁰⁰, R. Kopeliansky⁴², S. Koperny^{87a}, K. Korcyl⁸⁸, K. Kordas^{156,e}, A. Korn⁹⁸, S. Korn⁵⁶, I. Korolkov¹³, N. Korotkova³⁸, B. Kortman¹¹⁷, O. Kortner¹¹², S. Kortner¹¹², W. H. Kostecka¹¹⁸, V. V. Kostyukhin¹⁴⁵, A. Kotsokechagia³⁷, A. Kotwal⁵², A. Koulouris³⁷, A. Kourkoumeli-Charalampidi^{74a,74b}, C. Kourkoumelis⁹, E. Kourlitis¹¹², O. Kovanda¹²⁶, R. Kowalewski¹⁶⁸, W. Kozanecki¹²⁶, A. S. Kozhin³⁸, V. A. Kramarenko³⁸, G. Kramberger⁹⁵, P. Kramer¹⁰², M. W. Krasny¹³⁰, A. Krasznahorkay³⁷, A. C. Kraus¹¹⁸, J. W. Kraus¹⁷⁴, J. A. Kremer⁴⁹, T. Kresse⁵¹, L. Kretschmann¹⁷⁴, J. Kretzschmar⁹⁴, K. Kreul¹⁹, P. Krieger¹⁵⁸, M. Krivos¹³⁶, K. Krizka²¹, K. Kroeninger⁵⁰, H. Kroha¹¹², J. Kroll¹³⁴, J. Kroll¹³¹, K. S. Krowpman¹⁰⁹, U. Kruchonak³⁹, H. Krüger²⁵, N. Krumnack⁸², M. C. Kruse⁵², O. Kuchinskaia³⁸, S. Kuday^{3a}, S. Kuehn³⁷, R. Kuesters⁵⁵, T. Kuhl⁴⁹, V. Kukhtin³⁹, Y. Kulchitsky^{38,a}, S. Kuleshov^{140b,140d}, M. Kumar^{34g}, N. Kumari⁴⁹, P. Kumari^{159b}, A. Kupco¹³⁴, T. Kupfer⁵⁰, A. Kupich³⁸, O. Kuprash⁵⁵, H. Kurashige⁸⁶, L. L. Kurchaninov^{159a}, O. Kurdysh⁶⁷, Y. A. Kurochkin³⁸, A. Kurova³⁸, M. Kuze¹⁴¹, A. K. Kvam¹⁰⁵, J. Kvita¹²⁵, T. Kwan¹⁰⁶, N. G. Kyriacou¹⁰⁸, L. A. O. Laatu¹⁰⁴, C. Lacasta¹⁶⁶, F. Lacava^{76a,76b}, H. Lacker¹⁹, D. Lacour¹³⁰, N. N. Lad⁹⁸, E. Ladygin³⁹, A. Lafarge⁴¹, B. Laforge¹³⁰, T. Lagouri¹⁷⁵, F. Z. Lahbab^{36a}, S. Lai⁵⁶, J. E. Lambert¹⁶⁸, S. Lammers⁶⁹, W. Lampi⁷, C. Lampoudis^{156,e}, G. Lamprinoudis¹⁰², A. N. Lancaster¹¹⁸, E. Lançon³⁰, U. Landgraf⁵⁵, M. P. J. Landon⁹⁶, V. S. Lang⁵⁵, O. K. B. Langrekken¹²⁸, A. J. Lankford¹⁶², F. Lanni³⁷, K. Lantzsch²⁵, A. Lanza^{74a}, M. Lanzac Berrocal¹⁶⁶, J. F. Laporte¹³⁸, T. Lari^{72a}, F. Lasagni Manghi^{24b}, M. Lassnig³⁷, V. Latonova¹³⁴, A. Laurier¹⁵⁴, S. D. Lawlor¹⁴³, Z. Lawrence¹⁰³, R. Lazaridou¹⁷⁰, M. Lazzaroni^{72a,72b}, B. Le¹⁰³, H. D. M. Le¹⁰⁹, E. M. Le Boulicau⁵², L. T. Le Pottier^{18a}, B. Leban^{24a,24b}, A. Lebedev⁸², M. LeBlanc¹⁰³, F. Ledroit-Guillon⁶¹, S. C. Lee¹⁵², S. Lee^{48a,48b}, T. F. Lee⁹⁴, L. L. Leeuw^{34c}, H. P. Lefebvre⁹⁷, M. Lefebvre¹⁶⁸, C. Leggett^{18a}, G. Lehmann Miotto³⁷, M. Leigh⁵⁷, W. A. Leight¹⁰⁵, W. Leinonen¹¹⁶, A. Leisos^{156,t}, M. A. L. Leite^{84c}, C. E. Leitgeb¹⁹, R. Leitner¹³⁶, K. J. C. Leney⁴⁵, T. Lenz²⁵, S. Leone^{75a}, C. Leonidopoulos⁵³, A. Leopold¹⁴⁸, R. Les¹⁰⁹, C. G. Lester³³, M. Levchenko³⁸, J. Levêque⁴, L. J. Levinson¹⁷², G. Levirini^{24a,24b}, M. P. Lewicki⁸⁸, C. Lewis¹⁴², D. J. Lewis⁴, L. Lewitt¹⁴³, A. Li⁵, B. Li^{63b}, C. Li^{63a}, C-Q. Li¹¹², H. Li^{63a}, H. Li^{63b}, H. Li^{114a}, H. Li¹⁵, H. Li^{63b}, J. Li^{63c}, K. Li¹⁴, L. Li^{63c}, M. Li^{14,114c}, S. Li^{14,114c}, S. Li^{63c,63d}, T. Li⁵, X. Li¹⁰⁶, Z. Li¹²⁹, Z. Li¹⁵⁷, Z. Li^{14,114c}, Z. Li^{63a}, S. Liang^{14,114c}, Z. Liang¹⁴, M. Liberatore¹³⁸, B. Liberti^{77a}, K. Lie^{65c}, J. Lieber Marin^{84e}, H. Lien⁶⁹, H. Lin¹⁰⁸, K. Lin¹⁰⁹, R. E. Lindley⁷, J. H. Lindon², J. Ling⁶², E. Lipeles¹³¹, A. Lipniacka¹⁷, A. Lister¹⁶⁷, J. D. Little⁶⁹, B. Liu¹⁴, B. X. Liu^{114b}, D. Liu^{63c,63d}, E. H. L. Liu²¹, J. B. Liu^{63a}, J. K. K. Liu³³, K. Liu^{63d}, K. Liu^{63c,63d}, M. Liu^{63a}, M. Y. Liu^{63a}, P. Liu¹⁴, Q. Liu^{63c,63d,142}, X. Liu^{63a}, X. Liu^{63b}, Y. Liu^{114b,114c}, Y. L. Liu^{63b}, Y. W. Liu^{63a}, S. L. Lloyd⁹⁶, E. M. Lobodzinska⁴⁹, P. Loch⁷, T. Lohse¹⁹, K. Lohwasser¹⁴³, E. Loiacono⁴⁹, M. Lokajicek^{134,*}, J. D. Lomas²¹, J. D. Long¹⁶⁵, I. Longarini¹⁶², R. Longo¹⁶⁵,

- I. Lopez Paz⁶⁸, A. Lopez Solis⁴⁹, N. A. Lopez-canelas⁷, N. Lorenzo Martinez⁴, A. M. Lory¹¹¹, M. Losada^{119a}, G. Löscheke Centeno¹⁵⁰, O. Loseva³⁸, X. Lou^{48a,48b}, X. Lou^{14,114c}, A. Lounis⁶⁷, P. A. Love⁹³, G. Lu^{14,114c}, M. Lu⁶⁷, S. Lu¹³¹, Y. J. Lu⁶⁶, H. J. Lubatti¹⁴², C. Luci^{76a,76b}, F. L. Lucio Alves^{114a}, F. Luehring⁶⁹, I. Luise¹⁴⁹, O. Lukianchuk⁶⁷, O. Lundberg¹⁴⁸, B. Lund-Jensen^{148,*}, N. A. Luongo⁶, M. S. Lutz³⁷, A. B. Lux²⁶, D. Lynn³⁰, R. Lysak¹³⁴, E. Lytken¹⁰⁰, V. Lyubushkin³⁹, T. Lyubushkina³⁹, M. M. Lyukova¹⁴⁹, M. Firdaus M. Soberi⁵³, H. Ma³⁰, K. Ma^{63a}, L. L. Ma^{63b}, W. Ma^{63a}, Y. Ma¹²⁴, J. C. MacDonald¹⁰², P. C. Machado De Abreu Farias^{84e}, R. Madar⁴¹, T. Madula⁹⁸, J. Maeda⁸⁶, T. Maeno³⁰, H. Maguire¹⁴³, V. Maiboroda¹³⁸, A. Maio^{133a,133b,133d}, K. Maj^{87a}, O. Majersky⁴⁹, S. Majewski¹²⁶, N. Makovec⁶⁷, V. Maksimovic¹⁶, B. Malaeșcu¹³⁰, Pa. Malecki⁸⁸, V. P. Maleev³⁸, F. Malek^{61,o}, M. Mali⁹⁵, D. Malito⁹⁷, U. Mallik^{81,*}, S. Maltezos¹⁰, S. Malyukov³⁹, J. Mamuzic¹³, G. Mancini⁵⁴, M. N. Mancini²⁷, G. Manco^{74a,74b}, J. P. Mandalia⁹⁶, S. S. Mandarry¹⁵⁰, I. Mandić⁹⁵, L. Manhaes de Andrade Filho^{84a}, I. M. Maniatis¹⁷², J. Manjarres Ramos⁹¹, D. C. Mankad¹⁷², A. Mann¹¹¹, S. Manzoni³⁷, L. Mao^{63c}, X. Mapekula^{34c}, A. Marantis^{156,t}, G. Marchiori⁵, M. Marcisovsky¹³⁴, C. Marcon^{72a}, M. Marinescu²¹, S. Marium⁴⁹, M. Marjanovic¹²³, A. Markhoos⁵⁵, M. Markovitch⁶⁷, E. J. Marshall¹⁹³, Z. Marshall^{18a}, S. Marti-Garcia¹⁶⁶, J. Martin⁹⁸, T. A. Martin¹³⁷, V. J. Martin⁵³, B. Martin dit Latour¹⁷, L. Martinelli^{76a,76b}, M. Martinez^{13,u}, P. Martinez Agullo¹⁶⁶, V. I. Martinez Outschoorn¹⁰⁵, P. Martinez Suarez¹³, S. Martin-Haugh¹³⁷, G. Martinovicova¹³⁶, V. S. Martouiu^{28b}, A. C. Martyniuk⁹⁸, A. Marzin³⁷, D. Mascione^{79a,79b}, L. Masetti¹⁰², J. Masik¹⁰³, A. L. Maslennikov³⁸, P. Massarotti^{73a,73b}, P. Mastrandrea^{75a,75b}, A. Mastroberardino^{44a,44b}, T. Masubuchi¹²⁷, T. T. Mathew¹²⁶, T. Mathisen¹⁶⁴, J. Matousek¹³⁶, J. Maurer^{28b}, T. Maurin⁶⁰, A. J. Maury⁶⁷, B. Maček⁹⁵, D. A. Maximov³⁸, A. E. May¹⁰³, R. Mazini¹⁵², I. Maznás¹¹⁸, M. Mazza¹⁰⁹, S. M. Mazza¹³⁹, E. Mazzeo^{72a,72b}, C. Mc Ginn³⁰, J. P. Mc Gowan¹⁶⁸, S. P. Mc Kee¹⁰⁸, C. C. McCracken¹⁶⁷, E. F. McDonald¹⁰⁷, A. E. McDougall¹¹⁷, J. A. Mcfayden¹⁵⁰, R. P. McGovern¹³¹, R. P. McKenzie^{34g}, T. C. McLachlan⁴⁹, D. J. McLaughlin⁹⁸, S. J. McMahon¹³⁷, C. M. Mcpartland⁹⁴, R. A. McPherson^{168,y}, S. Mehlhase¹¹¹, A. Mehta⁹⁴, D. Melini¹⁶⁶, B. R. Mellado Garcia^{34g}, A. H. Melo⁵⁶, F. Meloni⁴⁹, A. M. Mendes Jacques Da Costa¹⁰³, H. Y. Meng¹⁵⁸, L. Meng⁹³, S. Menke¹¹², M. Mentink³⁷, E. Meoni^{44a,44b}, G. Mercado¹¹⁸, S. Merianos¹⁵⁶, C. Merlassino^{70a,70c}, L. Merola^{73a,73b}, C. Meroni^{72a,72b}, J. Metcalfe⁶, A. S. Mete⁶, E. Meuser¹⁰², C. Meyer⁶⁹, J-P. Meyer¹³⁸, R. P. Middleton¹³⁷, L. Mijovic⁵³, G. Mikenberg¹⁷², M. Mikestikova¹³⁴, M. Mikuž⁹⁵, H. Mildner¹⁰², A. Milic³⁷, D. W. Miller⁴⁰, E. H. Miller¹⁴⁷, L. S. Miller³⁵, A. Milov¹⁷², D. A. Milstead^{48a,48b}, T. Min^{114a}, A. A. Minaenko³⁸, I. A. Minashvili^{153b}, L. Mince⁶⁰, A. I. Mincer¹²⁰, B. Mindur^{87a}, M. Mineev³⁹, Y. Mino⁸⁹, L. M. Mir¹³, M. Miralles Lopez⁶⁰, M. Mironova^{18a}, M. C. Missio¹¹⁶, A. Mitra¹⁷⁰, V. A. Mitsou¹⁶⁶, Y. Mitsumori¹¹³, O. Miu¹⁵⁸, P. S. Miyagawa⁹⁶, T. Mkrtchyan^{64a}, M. Mlinarevic⁹⁸, T. Mlinarevic⁹⁸, M. Mlynarikova³⁷, S. Mobius²⁰, P. Mogg¹¹¹, M. H. Mohamed Farook¹¹⁵, A. F. Mohammed^{14,114c}, S. Mohapatra⁴², G. Mokgatitswane^{34g}, L. Moleri¹⁷², B. Mondal¹⁴⁵, S. Mondal¹³⁵, K. Mönig⁴⁹, E. Monnier¹⁰⁴, L. Monsonis Romero¹⁶⁶, J. Montejano Berlingen¹³, A. Montella^{48a,48b}, M. Montella¹²², F. Montereali^{78a,78b}, F. Monticelli⁹², S. Monzani^{70a,70c}, A. Morancho Tarda⁴³, N. Morange⁶⁷, A. L. Moreira De Carvalho⁴⁹, M. Moreno Llácer¹⁶⁶, C. Moreno Martinez⁵⁷, J. M. Moreno Perez^{23b}, P. Morettini^{58b}, S. Morgenstern³⁷, M. Morii⁶², M. Morinaga¹⁵⁷, F. Morodei^{76a,76b}, L. Morvaj³⁷, P. Moschovakos³⁷, B. Moser¹²⁹, M. Mosidze^{153b}, T. Moskalets⁴⁵, P. Moskvitina¹¹⁶, J. Moss^{32,l}, P. Moszkowicz^{87a}, A. Moussa^{36d}, E. J. W. Moyse¹⁰⁵, O. Mtintsilana^{34g}, S. Muanza¹⁰⁴, J. Mueller¹³², D. Muenstermann⁹³, R. Müller³⁷, G. A. Mullier¹⁶⁴, A. J. Mullin³³, J. J. Mullin¹³¹, D. P. Mungo¹⁵⁸, D. Munoz Perez¹⁶⁶, F. J. Munoz Sanchez¹⁰³, M. Murin¹⁰³, W. J. Murray^{137,170}, M. Muškinja⁹⁵, C. Mwewa³⁰, A. G. Myagkov^{38,a}, A. J. Myers⁸, G. Myers¹⁰⁸, M. Myska¹³⁵, B. P. Nachman^{18a}, O. Nackenhorst⁵⁰, K. Nagai¹²⁹, K. Nagano⁸⁵, R. Nagasaka¹⁵⁷, J. L. Nagle^{30,ah}, E. Nagy¹⁰⁴, A. M. Nairz³⁷, Y. Nakahama⁸⁵, K. Nakamura⁸⁵, K. Nakkalil⁵, H. Nanjo¹²⁷, E. A. Narayanan¹¹⁵, I. Naryshkin³⁸, L. Nasella^{72a,72b}, M. Naseri³⁵, S. Nasri^{119b}, C. Nass²⁵, G. Navarro^{23a}, J. Navarro-Gonzalez¹⁶⁶, R. Nayak¹⁵⁵, A. Nayaz¹⁹, P. Y. Nechaeva³⁸, S. Nechaeva^{24a,24b}, F. Nechansky⁴⁹, L. Nedic¹²⁹, T. J. Neep²¹, A. Negri^{74a,74b}, M. Negrini^{24b}, C. Nellist¹¹⁷, C. Nelson¹⁰⁶, K. Nelson¹⁰⁸, S. Nemecek¹³⁴, M. Nessi^{37,i}, M. S. Neubauer¹⁶⁵, F. Neuhaus¹⁰², J. Neundorf⁴⁹, J. Newell⁹⁴, P. R. Newman²¹, C. W. Ng¹³², Y. W. Y. Ng⁴⁹, B. Ngair^{119a}, H. D. N. Nguyen¹¹⁰, R. B. Nickerson¹²⁹, R. Nicolaïdou¹³⁸, J. Nielsen¹³⁹, M. Niemeyer⁵⁶, J. Niermann⁵⁶, N. Nikiforou³⁷, V. Nikolaenko^{38,a}, I. Nikolic-Audit¹³⁰, K. Nikolopoulos²¹, P. Nilsson³⁰, I. Ninca⁴⁹, G. Ninio¹⁵⁵, A. Nisati^{76a}, N. Nishu², R. Nisius¹¹², J-E. Nitschke⁵¹, E. K. Nkadimeng^{34g}, T. Nobe¹⁵⁷, T. Nommensen¹⁵¹, M. B. Norfolk¹⁴³, B. J. Norman³⁵, M. Noury^{36a}, J. Novak⁹⁵, T. Novak⁹⁵, L. Novotny¹³⁵, R. Novotny¹¹⁵, L. Nozka¹²⁵

- K. Ntekas¹⁶², N. M. J. Nunes De Moura Junior^{84b}, J. Ocariz¹³⁰, A. Ochi⁸⁶, I. Ochoa^{133a}, S. Oerdeke^{49,v}, J. T. Offermann⁴⁰, A. Ogrodnik¹³⁶, A. Oh¹⁰³, C. C. Ohm¹⁴⁸, H. Oide⁸⁵, R. Oishi¹⁵⁷, M. L. Ojeda⁴⁹, Y. Okumura¹⁵⁷, L. F. Oleiro Seabra^{133a}, I. Oleksiyuk⁵⁷, S. A. Olivares Pino^{140d}, G. Oliveira Correa¹³, D. Oliveira Damazio³⁰, J. L. Oliver¹⁶², Ö. O. Öncel⁵⁵, A. P. O'Neill²⁰, A. Onofre^{133a,133e}, P. U. E. Onyisi¹¹, M. J. Oreglia⁴⁰, G. E. Orellana⁹², D. Orestano^{78a,78b}, N. Orlando¹³, R. S. Orr¹⁵⁸, L. M. Osojnak¹³¹, R. Ospanov^{63a}, G. Otero y Garzon³¹, H. Otono⁹⁰, P. S. Ott^{64a}, G. J. Ottino^{18a}, M. Ouchrif^{36d}, F. Ould-Saada¹²⁸, T. Ovsiannikova¹⁴², M. Owen⁶⁰, R. E. Owen¹³⁷, V. E. Ozcan^{22a}, F. Ozturk⁸⁸, N. Ozturk⁸, S. Ozturk⁸³, H. A. Pacey¹²⁹, A. Pacheco Pages¹³, C. Padilla Aranda¹³, G. Padovano^{76a,76b}, S. Pagan Griso^{18a}, G. Palacino⁶⁹, A. Palazzo^{71a,71b}, J. Pampel²⁵, J. Pan¹⁷⁵, T. Pan^{65a}, D. K. Panchal¹¹, C. E. Pandini¹¹⁷, J. G. Panduro Vazquez¹³⁷, H. D. Pandya¹, H. Pang¹⁵, P. Pani⁴⁹, G. Panizzo^{70a,70c}, L. Panwar¹³⁰, L. Paolozzi⁵⁷, S. Parajuli¹⁶⁵, A. Paramonov⁶, C. Paraskevopoulos⁵⁴, D. Paredes Hernandez^{65b}, A. Paret^{74a,74b}, K. R. Park⁴², T. H. Park¹⁵⁸, M. A. Parker³³, F. Parodi^{58a,58b}, E. W. Parrish¹¹⁸, V. A. Parrish⁵³, J. A. Parsons⁴², U. Parzefall⁵⁵, B. Pascual Dias¹¹⁰, L. Pascual Dominguez¹⁰¹, E. Pasqualucci^{76a}, S. Passaggio^{58b}, F. Pastore⁹⁷, P. Patel⁸⁸, U. M. Patel⁵², J. R. Pater¹⁰³, T. Pauly³⁷, C. I. Pazos¹⁶¹, J. Pearkes¹⁴⁷, M. Pedersen¹²⁸, R. Pedro^{133a}, S. V. Peleganchuk³⁸, O. Penc³⁷, E. A. Pender⁵³, S. Peng¹⁵, G. D. Penn¹⁷⁵, K. E. Penski¹¹¹, M. Penzin³⁸, B. S. Peralva^{84d}, A. P. Pereira Peixoto¹⁴², L. Pereira Sanchez¹⁴⁷, D. V. Perpelitsa^{30,ah}, G. Perera¹⁰⁵, E. Perez Codina^{159a}, M. Perganti¹⁰, H. Pernegger³⁷, S. Perrella^{76a,76b}, O. Perrin⁴¹, K. Peters⁴⁹, R. F. Y. Peters¹⁰³, B. A. Petersen³⁷, T. C. Petersen⁴³, E. Petit¹⁰⁴, V. Petousis¹³⁵, C. Petridou^{156,e}, T. Petru¹³⁶, A. Petrukhin¹⁴⁵, M. Pettee^{18a}, A. Petukhov³⁸, K. Petukhova³⁷, R. Pezoa^{140f}, L. Pezzotti³⁷, G. Pezzullo¹⁷⁵, T. M. Pham¹⁷³, T. Pham¹⁰⁷, P. W. Phillips¹³⁷, G. Piacquadio¹⁴⁹, E. Pianori^{18a}, F. Piazza¹²⁶, R. Piegaia³¹, D. Pietreanu^{28b}, A. D. Pilkington¹⁰³, M. Pinamonti^{70a,70c}, J. L. Pinfold², B. C. Pinheiro Pereira^{133a}, J. Pinol Bel¹³, A. E. Pinto Pinoargote¹³⁸, L. Pintucci^{70a,70c}, K. M. Piper¹⁵⁰, A. Pirttikoski⁵⁷, D. A. Pizzi³⁵, L. Pizzimento^{65b}, A. Pizzini¹¹⁷, M.-A. Pleier³⁰, V. Pleskot¹³⁶, E. Plotnikova³⁹, G. Poddar⁹⁶, R. Poettgen¹⁰⁰, L. Poggioli¹³⁰, I. Pokharel⁵⁶, S. Polacek¹³⁶, G. Polesello^{74a}, A. Poley^{146,159a}, A. Polini^{24b}, C. S. Pollard¹⁷⁰, Z. B. Pollock¹²², E. Pompa Pacchi^{76a,76b}, N. I. Pond⁹⁸, D. Ponomarenko⁶⁹, L. Pontecorvo³⁷, S. Popa^{28a}, G. A. Popeneicu^{28d}, A. Poreba³⁷, D. M. Portillo Quintero^{159a}, S. Pospisil¹³⁵, M. A. Postill¹⁴³, P. Postolache^{28c}, K. Potamianos¹⁷⁰, P. A. Potepa^{87a}, I. N. Potrap³⁹, C. J. Potter³³, H. Potti¹⁵¹, J. Poveda¹⁶⁶, M. E. Pozo Astigarraga³⁷, A. Prades Ibanez^{77a,77b}, J. Pretel¹⁶⁸, D. Price¹⁰³, M. Primavera^{71a}, L. Primomo^{70a,70c}, M. A. Principe Martin¹⁰¹, R. Privara¹²⁵, T. Procter⁶⁰, M. L. Proffitt¹⁴², N. Proklova¹³¹, K. Prokofiev^{65c}, G. Proto¹¹², J. Proudfoot⁶, M. Przybycien^{87a}, W. W. Przygoda^{87b}, A. Psallidas⁴⁷, J. E. Puddefoot¹⁴³, D. Pudzha⁵⁵, D. Pyatitzibyanseva³⁸, J. Qian¹⁰⁸, D. Qichen¹⁰³, Y. Qin¹³, T. Qiu⁵³, A. Quadt⁵⁶, M. Queitsch-Maitland¹⁰³, G. Quetant⁵⁷, R. P. Quinn¹⁶⁷, G. Rabanal Bolanos⁶², D. Rafanoharana⁵⁵, F. Raffaeli^{77a,77b}, F. Ragusa^{72a,72b}, J. L. Rainbolt⁴⁰, J. A. Raine⁵⁷, S. Rajagopalan³⁰, E. Ramakoti³⁸, L. Rambelli^{58a,58b}, I. A. Ramirez-Berend³⁵, K. Ran^{49,114c}, D. S. Rankin¹³¹, N. P. Rapheeha^{34g}, H. Rasheed^{28b}, V. Raskina¹³⁰, D. F. Rassloff^{64a}, A. Rastogi^{18a}, S. Rave¹⁰², S. Ravera^{58a,58b}, B. Ravina⁵⁶, I. Ravinovich¹⁷², M. Raymond³⁷, A. L. Read¹²⁸, N. P. Readioff¹⁴³, D. M. Rebuzzi^{74a,74b}, G. Redlinger³⁰, A. S. Reed¹¹², K. Reeves²⁷, J. A. Reidelsturz¹⁷⁴, D. Reikher¹²⁶, A. Rej⁵⁰, C. Rembser³⁷, M. Renda^{28b}, F. Renner⁴⁹, A. G. Rennie¹⁶², A. L. Rescia⁴⁹, S. Resconi^{72a}, M. Ressegotti^{58a,58b}, S. Rettie³⁷, J. G. Reyes Rivera¹⁰⁹, E. Reynolds^{18a}, O. L. Rezanova³⁸, P. Reznicek¹³⁶, H. Riani^{36d}, N. Ribaric⁹³, E. Ricci^{79a,79b}, R. Richter¹¹², S. Richter^{48a,48b}, E. Richter-Was^{87b}, M. Ridel¹³⁰, S. Ridouani^{36d}, P. Rieck¹²⁰, P. Riedler³⁷, E. M. Riefel^{48a,48b}, J. O. Rieger¹¹⁷, M. Rijssenbeek¹⁴⁹, M. Rimoldi³⁷, L. Rinaldi^{24a,24b}, P. Rincke⁵⁶, T. T. Rinn³⁰, M. P. Rinnagel¹¹¹, G. Ripellino¹⁶⁴, I. Riu¹³, J. C. Rivera Vergara¹⁶⁸, F. Rizatdinova¹²⁴, E. Rizvi⁹⁶, B. R. Roberts^{18a}, S. S. Roberts¹³⁹, S. H. Robertson^{106,y}, D. Robinson³³, M. Robles Manzano¹⁰², A. Robson⁶⁰, A. Rocchi^{77a,77b}, C. Roda^{75a,75b}, S. Rodriguez Bosca³⁷, Y. Rodriguez Garcia^{23a}, A. Rodriguez Rodriguez⁵⁵, A. M. Rodriguez Vera¹¹⁸, S. Roe³⁷, J. T. Roemer³⁷, A. R. Roepe-Gier¹³⁹, O. Røhne¹²⁸, R. A. Rojas¹⁰⁵, C. P. A. Roland¹³⁰, J. Roloff³⁰, A. Romaniouk³⁸, E. Romano^{74a,74b}, M. Romano^{24b}, A. C. Romero Hernandez¹⁶⁵, N. Rompotis⁹⁴, L. Roos¹³⁰, S. Rosati^{76a}, B. J. Rosser⁴⁰, E. Rossi¹²⁹, E. Rossi^{73a,73b}, L. P. Rossi⁶², L. Rossini⁵⁵, R. Rosten¹²², M. Rotaru^{28b}, B. Rottler⁵⁵, C. Rougier⁹¹, D. Rousseau⁶⁷, D. Rousso⁴⁹, A. Roy¹⁶⁵, S. Roy-Garand¹⁵⁸, A. Rozanov¹⁰⁴, Z. M. A. Rozario⁶⁰, Y. Rozen¹⁵⁴, A. Rubio Jimenez¹⁶⁶, A. J. Ruby⁹⁴, V. H. Ruelas Rivera¹⁹, T. A. Ruggeri¹, A. Ruggiero¹²⁹, A. Ruiz-Martinez¹⁶⁶, A. Rummler³⁷, Z. Rurikova⁵⁵, N. A. Rusakovich³⁹, H. L. Russell¹⁶⁸, G. Russo^{76a,76b}, J. P. Rutherford Foord⁷, S. Rutherford Colmenares³³, M. Rybar¹³⁶, E. B. Rye¹²⁸, A. Ryzhov⁴⁵, J. A. Sabater Iglesias⁵⁷, H.-F.-W. Sadrozinski¹³⁹, F. Safai Tehrani^{76a},

- B. Safarzadeh Samani¹³⁷, S. Saha¹, M. Sahinsoy⁸³, A. Saibel¹⁶⁶, M. Saimpert¹³⁸, M. Saito¹⁵⁷, T. Saito¹⁵⁷, A. Sala^{72a,72b}, D. Salamani³⁷, A. Salnikov¹⁴⁷, J. Salt¹⁶⁶, A. Salvador Salas¹⁵⁵, D. Salvatore^{44a,44b}, F. Salvatore¹⁵⁰, A. Salzburger³⁷, D. Sammel⁵⁵, E. Sampson⁹³, D. Sampsonidis^{156,c}, D. Sampsonidou¹²⁶, J. Sánchez¹⁶⁶, V. Sanchez Sebastian¹⁶⁶, H. Sandaker¹²⁸, C. O. Sander⁴⁹, J. A. Sandesara¹⁰⁵, M. Sandhoff¹⁷⁴, C. Sandoval^{23b}, L. Sanfilippo^{64a}, D. P. C. Sankey¹³⁷, T. Sano⁸⁹, A. Sansoni⁵⁴, L. Santi^{37,76b}, C. Santoni⁴¹, H. Santos^{133a,133b}, A. Santra¹⁷², E. Sanzani^{24a,24b}, K. A. Saoucha¹⁶³, J. G. Saraiva^{133a,133d}, J. Sardain⁷, O. Sasaki⁸⁵, K. Sato¹⁶⁰, C. Sauer^{64b}, E. Sauvan⁴, P. Savard^{158,af}, R. Sawada¹⁵⁷, C. Sawyer¹³⁷, L. Sawyer⁹⁹, C. Sbarra^{24b}, A. Sbrizzi^{24a,24b}, T. Scanlon⁹⁸, J. Schaarschmidt¹⁴², U. Schäfer¹⁰², A. C. Schaffer^{45,67}, D. Schaile¹¹¹, R. D. Schamberger¹⁴⁹, C. Scharf¹⁹, M. M. Schefer²⁰, V. A. Schegelsky³⁸, D. Scheirich¹³⁶, M. Schernau¹⁶², C. Scheulen⁵⁶, C. Schiavi^{58a,58b}, M. Schioppa^{44a,44b}, B. Schlag¹⁴⁷, K. E. Schleicher⁵⁵, S. Schlenker³⁷, J. Schmeing¹⁷⁴, M. A. Schmidt¹⁷⁴, K. Schmieden¹⁰², C. Schmitt¹⁰², N. Schmitt¹⁰², S. Schmitt⁴⁹, L. Schoeffel¹³⁸, A. Schoening^{64b}, P. G. Scholer³⁵, E. Schopf¹²⁹, M. Schott²⁵, J. Schovancova³⁷, S. Schramm⁵⁷, T. Schroer⁵⁷, H-C. Schultz-Coulon^{64a}, M. Schumacher⁵⁵, B. A. Schumm¹³⁹, Ph. Schune¹³⁸, A. J. Schuy¹⁴², H. R. Schwartz¹³⁹, A. Schwartzman¹⁴⁷, T. A. Schwarz¹⁰⁸, Ph. Schwemling¹³⁸, R. Schwienhorst¹⁰⁹, F. G. Sciacca²⁰, A. Sciandra³⁰, G. Sciolla²⁷, F. Scuri^{75a}, C. D. Sebastiani⁹⁴, K. Sedlaczek¹¹⁸, S. C. Seidel¹¹⁵, A. Seiden¹³⁹, B. D. Seidlitz⁴², C. Seitz⁴⁹, J. M. Seixas^{84b}, G. Sekhniaidze^{73a}, L. Selem⁶¹, N. Semprini-Cesari^{24a,24b}, D. Sengupta⁵⁷, V. Senthilkumar¹⁶⁶, L. Serin⁶⁷, M. Sessa^{77a,77b}, H. Severini¹²³, F. Sforza^{58a,58b}, A. Sfyrla⁵⁷, Q. Sha¹⁴, E. Shabalina⁵⁶, A. H. Shah³³, R. Shaheen¹⁴⁸, J. D. Shahinian¹³¹, D. Shaked Renous¹⁷², L. Y. Shan¹⁴, M. Shapiro^{18a}, A. Sharma³⁷, A. S. Sharma¹⁶⁷, P. Sharma⁸¹, P. B. Shatalov³⁸, K. Shaw¹⁵⁰, S. M. Shaw¹⁰³, Q. Shen^{63c}, D. J. Sheppard¹⁴⁶, P. Sherwood⁹⁸, L. Shi⁹⁸, X. Shi¹⁴, S. Shimizu⁸⁵, C. O. Shimmin¹⁷⁵, J. D. Shinner⁹⁷, I. P. J. Shipsey^{129,*}, S. Shirabe⁹⁰, M. Shiyakova^{39,w}, M. J. Shochet⁴⁰, D. R. Shope¹²⁸, B. Shrestha¹²³, S. Shrestha^{122,ai}, M. J. Shroff¹⁶⁸, P. Sicho¹³⁴, A. M. Sickles¹⁶⁵, E. Sideras Haddad^{34g}, A. C. Sidley¹¹⁷, A. Sidoti^{24b}, F. Siegert⁵¹, Dj. Sijacki¹⁶, F. Sili⁹², J. M. Silva⁵³, I. Silva Ferreira^{84b}, M. V. Silva Oliveira³⁰, S. B. Silverstein^{48a}, S. Simion⁶⁷, R. Simoniello³⁷, E. L. Simpson¹⁰³, H. Simpson¹⁵⁰, L. R. Simpson¹⁰⁸, N. D. Simpson¹⁰⁰, S. Simsek⁸³, S. Sindhu⁵⁶, P. Sinervo¹⁵⁸, S. Singh¹⁵⁸, S. Sinha⁴⁹, S. Sinha¹⁰³, M. Sioli^{24a,24b}, I. Siral³⁷, E. Sitnikova⁴⁹, J. Sjölin^{48a,48b}, A. Skaf⁵⁶, E. Skorda²¹, P. Skubic¹²³, M. Slawinska⁸⁸, V. Smakhtin¹⁷², B. H. Smart¹³⁷, S. Yu. Smirnov³⁸, Y. Smirnov³⁸, L. N. Smirnova^{38,a}, O. Smirnova¹⁰⁰, A. C. Smith⁴², D. R. Smith¹⁶², E. A. Smith⁴⁰, J. L. Smith¹⁰³, R. Smith¹⁴⁷, M. Smizanska⁹³, K. Smolek¹³⁵, A. A. Snesarev³⁸, S. R. Snider¹⁵⁸, H. L. Snoek¹¹⁷, S. Snyder³⁰, R. Sobie^{168,y}, A. Soffer¹⁵⁵, C. A. Solans Sanchez³⁷, E. Yu. Soldatov³⁸, U. Soldevila¹⁶⁶, A. A. Solodkov³⁸, S. Solomon²⁷, A. Soloshenko³⁹, K. Solovieva⁵⁵, O. V. Solovyanov⁴¹, P. Sommer⁵¹, A. Sonay¹³, W. Y. Song^{159b}, A. Sopczak¹³⁵, A. L. Sopio⁹⁸, F. Sopkova^{29b}, J. D. Sorenson¹¹⁵, I. R. Sotarriva Alvarez¹⁴¹, V. Sothilingam^{64a}, O. J. Soto Sandoval^{140b,140c}, S. Sottocornola⁶⁹, R. Soualah¹⁶³, Z. Soumaimi^{36e}, D. South⁴⁹, N. Soybelman¹⁷², S. Spagnolo^{71a,71b}, M. Spalla¹¹², D. Sperlich⁵⁵, G. Spigo³⁷, B. Spisso^{73a,73b}, D. P. Spiteri⁶⁰, M. Spousta¹³⁶, E. J. Staats³⁵, R. Stamen^{64a}, A. Stampekit²¹, M. Standke²⁵, E. Stancka⁸⁸, W. Stanek-Maslouska⁴⁹, M. V. Stange⁵¹, B. Stanislaus^{18a}, M. M. Stanitzki⁴⁹, B. Stapi⁴⁹, E. A. Starchenko³⁸, G. H. Stark¹³⁹, J. Stark⁹¹, P. Staroba¹³⁴, P. Starovoitov^{64a}, S. Stärz¹⁰⁶, R. Staszewski⁸⁸, G. Stavropoulos⁴⁷, A. Steff³⁷, P. Steinberg³⁰, B. Stelzer^{146,159a}, H. J. Stelzer¹³², O. Stelzer-Chilton^{159a}, H. Stenzel⁵⁹, T. J. Stevenson¹⁵⁰, G. A. Stewart³⁷, J. R. Stewart¹²⁴, M. C. Stockton³⁷, G. Stoica^{28b}, M. Stolarski^{133a}, S. Stonjek¹¹², A. Straessner⁵¹, J. Strandberg¹⁴⁸, S. Strandberg^{48a,48b}, M. Stratmann¹⁷⁴, M. Strauss¹²³, T. Strebler¹⁰⁴, P. Strizenec^{29b}, R. Ströhmer¹⁶⁹, D. M. Strom¹²⁶, R. Stroynowski⁴⁵, A. Strubig^{48a,48b}, S. A. Stucci³⁰, B. Stugu¹⁷, J. Stupak¹²³, N. A. Styles⁴⁹, D. Su¹⁴⁷, S. Su^{63a}, W. Su^{63d}, X. Su^{63a}, D. Suchy^{29a}, K. Sugizaki¹⁵⁷, V. V. Sulin³⁸, M. J. Sullivan⁹⁴, D. M. S. Sultan¹²⁹, L. Sultanaliyeva³⁸, S. Sultansoy^{3b}, T. Sumida⁸⁹, S. Sun¹⁷³, O. Sunneborn Gudnadottir¹⁶⁴, N. Sur¹⁰⁴, M. R. Sutton¹⁵⁰, H. Suzuki¹⁶⁰, M. Svatos¹³⁴, M. Swiatlowski^{159a}, T. Swirski¹⁶⁹, I. Sykora^{29a}, M. Sykora¹³⁶, T. Sykora¹³⁶, D. Ta¹⁰², K. Tackmann^{49,v}, A. Taffard¹⁶², R. Tafirout^{159a}, J. S. Tafoya Vargas⁶⁷, Y. Takubo⁸⁵, M. Talby¹⁰⁴, A. A. Talyshев³⁸, K. C. Tam^{65b}, N. M. Tamir¹⁵⁵, A. Tanaka¹⁵⁷, J. Tanaka¹⁵⁷, R. Tanaka⁶⁷, M. Tanasini¹⁴⁹, Z. Tao¹⁶⁷, S. Tapia Araya^{140f}, S. Tapprogge¹⁰², A. Tarek Abouelfadl Mohamed¹⁰⁹, S. Tarem¹⁵⁴, K. Tariq¹⁴, G. Tarna^{28b}, G. F. Tartarelli^{72a}, M. J. Tartarin⁹¹, P. Tas¹³⁶, M. Tasevsky¹³⁴, E. Tassi^{44a,44b}, A. C. Tate¹⁶⁵, G. Tateno¹⁵⁷, Y. Tayalati^{36e,x}, G. N. Taylor¹⁰⁷, W. Taylor^{159b}, R. Teixeira De Lima¹⁴⁷, P. Teixeira-Dias⁹⁷, J. J. Teoh¹⁵⁸, K. Terashi¹⁵⁷, J. Terron¹⁰¹, S. Terzo¹³, M. Testa⁵⁴, R. J. Teuscher^{158,y}, A. Thaler⁸⁰, O. Theiner⁵⁷, N. Themistokleous⁵³, T. Theveneaux-Pelzer¹⁰⁴, O. Thielmann¹⁷⁴, D. W. Thomas⁹⁷,

- J. P. Thomas²¹, E. A. Thompson^{18a}, P. D. Thompson²¹, E. Thomson¹³¹, R. E. Thornberry⁴⁵, C. Tian^{63a}, Y. Tian⁵⁶, V. Tikhomirov^{38,a}, Yu.A. Tikhonov³⁸, S. Timoshenko³⁸, D. Timoshyn¹³⁶, E. X. L. Ting¹, P. Tipton¹⁷⁵, A. Tishelman-Charny³⁰, S. H. Tlou^{34g}, K. Todome¹⁴¹, S. Todorova-Nova¹³⁶, S. Todt⁵¹, L. Toffolin^{70a,70c}, M. Togawa⁸⁵, J. Tojo⁹⁰, S. Tokár^{29a}, K. Tokushuku⁸⁵, O. Toldaiev⁶⁹, M. Tomoto^{85,113}, L. Tompkins^{147,n}, K. W. Topolnicki^{87b}, E. Torrence¹²⁶, H. Torres⁹¹, E. Torró Pastor¹⁶⁶, M. Toscani³¹, C. Toscri⁴⁰, M. Tost¹¹, D. R. Tovey¹⁴³, I. S. Trandafir^{28b}, T. Trefzger¹⁶⁹, A. Tricoli³⁰, I. M. Trigger^{159a}, S. Trincaz-Duvoud¹³⁰, D. A. Trischuk²⁷, B. Trocmé⁶¹, A. Tropina³⁹, L. Truong^{34c}, M. Trzebinski⁸⁸, A. Trzupek⁸⁸, F. Tsai¹⁴⁹, M. Tsai¹⁰⁸, A. Tsiamis¹⁵⁶, P. V. Tsiareshka³⁸, S. Tsigaridas^{159a}, A. Tsirigotis^{156,t}, V. Tsiskaridze¹⁵⁸, E. G. Tskhadadze^{153a}, M. Tsopoulou¹⁵⁶, Y. Tsujikawa⁸⁹, I. I. Tsukerman³⁸, V. Tsulaia^{18a}, S. Tsuno⁸⁵, K. Tsuri¹²¹, D. Tsybychev¹⁴⁹, Y. Tu^{65b}, A. Tudorache^{28b}, V. Tudorache^{28b}, A. N. Tuna⁶², S. Turchikhin^{58a,58b}, I. Turk Cakir^{3a}, R. Turra^{72a}, T. Turtuvshin^{39,z}, P. M. Tuts⁴², S. Tzamarias^{156,e}, E. Tzovara¹⁰², F. Ukegawa¹⁶⁰, P. A. Ulloa Poblete^{140b,140c}, E. N. Umaka³⁰, G. Unal³⁷, A. Undrus³⁰, G. Unel¹⁶², J. Urban^{29b}, P. Urrejola^{140a}, G. Usai⁸, R. Ushioda¹⁴¹, M. Usman¹¹⁰, F. Ustuner⁵³, Z. Uysal⁸³, V. Vaccek¹³⁵, B. Vachon¹⁰⁶, T. Vafeiadis³⁷, A. Vaikus⁹⁸, C. Valderanis¹¹¹, E. Valdes Santurio^{48a,48b}, M. Valente^{159a}, S. Valentini^{24a,24b}, A. Valero¹⁶⁶, E. Valiente Moreno¹⁶⁶, A. Vallier⁹¹, J. A. Valls Ferrer¹⁶⁶, D. R. Van Arneman¹¹⁷, T. R. Van Daalen¹⁴², A. Van Der Graaf⁵⁰, P. Van Gemmeren⁶, M. Van Rijnbach³⁷, S. Van Stroud⁹⁸, I. Van Vulpen¹¹⁷, P. Vana¹³⁶, M. Vanadia^{77a,77b}, W. Vandelli³⁷, E. R. Vandewall¹²⁴, D. Vannicola¹⁵⁵, L. Vannoli⁵⁴, R. Vari^{76a}, E. W. Varnes⁷, C. Varni^{18b}, T. Varol¹⁵², D. Varouchas⁶⁷, L. Varriale¹⁶⁶, K. E. Varvell¹⁵¹, M. E. Vasile^{28b}, L. Vaslin⁸⁵, G. A. Vasquez¹⁶⁸, A. Vasyukov³⁹, L. M. Vaughan¹²⁴, R. Vavricka¹⁰², T. Vazquez Schroeder³⁷, J. Veatch³², V. Vecchio¹⁰³, M. J. Veen¹⁰⁵, I. Velisek³⁰, L. M. Veloce¹⁵⁸, F. Veloso^{133a,133c}, S. Veneziano^{76a}, A. Ventura^{71a,71b}, S. Ventura Gonzalez¹³⁸, A. Verbytskyi¹¹², M. Verducci^{75a,75b}, C. Vergis⁹⁶, M. Verissimo De Araujo^{84b}, W. Verkerke¹¹⁷, J. C. Vermeylen¹¹⁷, C. Vernieri¹⁴⁷, M. Vessella¹⁰⁵, M. C. Vetterli^{146,af}, A. Vgenopoulos¹⁰², N. Viaux Maira^{140f}, T. Vickey¹⁴³, O. E. Vickey Boeriu¹⁴³, G. H. A. Viehhauser¹²⁹, L. Vigani^{64b}, M. Vigl¹¹², M. Villa^{24a,24b}, M. Villaplana Perez¹⁶⁶, E. M. Villhauer⁵³, E. Vilucchi⁵⁴, M. G. Vinchter³⁵, A. Visibile¹¹⁷, C. Vittori³⁷, I. Vivarelli^{24a,24b}, E. Voevodina¹¹², F. Vogel¹¹¹, J. C. Voigt⁵¹, P. Vokac¹³⁵, Yu. Volkotrub^{87b}, J. Von Ahnen⁴⁹, E. Von Toerne²⁵, B. Vormwald³⁷, V. Vorobel¹³⁶, K. Vorobev³⁸, M. Vos¹⁶⁶, K. Voss¹⁴⁵, M. Vozak¹¹⁷, L. Vozdecky¹²³, N. Vranjes¹⁶, M. Vranjes Milosavljevic¹⁶, M. Vreeswijk¹¹⁷, N. K. Vu^{63c,63d}, R. Vuillermet³⁷, O. Vujinovic¹⁰², I. Vukotic⁴⁰, S. Wada¹⁶⁰, C. Wagner¹⁰⁵, J. M. Wagner^{18a}, W. Wagner¹⁷⁴, S. Wahdan¹⁷⁴, H. Wahlberg⁹², J. Walder¹³⁷, R. Walker¹¹¹, W. Walkowiak¹⁴⁵, A. Wall¹³¹, E. J. Wallin¹⁰⁰, T. Wamorkar⁶, A. Z. Wang¹³⁹, C. Wang¹⁰², C. Wang¹¹, H. Wang^{18a}, J. Wang^{65c}, P. Wang⁹⁸, R. Wang⁶², R. Wang⁶, S. M. Wang¹⁵², S. Wang^{63b}, S. Wang¹⁴, T. Wang^{63a}, W. T. Wang⁸¹, W. Wang¹⁴, X. Wang^{114a}, X. Wang¹⁶⁵, X. Wang^{63c}, Y. Wang^{63d}, Y. Wang^{114a}, Y. Wang^{63a}, Z. Wang¹⁰⁸, Z. Wang^{52,63c,63d}, Z. Wang¹⁰⁸, A. Warburton¹⁰⁶, R. J. Ward²¹, N. Warrack⁶⁰, S. Waterhouse⁹⁷, A. T. Watson²¹, H. Watson⁶⁰, M. F. Watson²¹, E. Watton^{60,137}, G. Watts¹⁴², B. M. Waugh⁹⁸, J. M. Webb⁵⁵, C. Weber³⁰, H. A. Weber¹⁹, M. S. Weber²⁰, S. M. Weber^{64a}, C. Wei^{63a}, Y. Wei⁵⁵, A. R. Weidberg¹²⁹, E. J. Weik¹²⁰, J. Weingarten⁵⁰, C. Weiser⁵⁵, C. J. Wells⁴⁹, T. Wenaus³⁰, B. Wendland⁵⁰, T. Wengler³⁷, N. S. Wenke¹¹², N. Wermes²⁵, M. Wessels^{64a}, A. M. Wharton⁹³, A. S. White⁶², A. White⁸, M. J. White¹, D. Whiteson¹⁶², L. Wickremasinghe¹²⁷, W. Wiedenmann¹⁷³, M. Wielers¹³⁷, C. Wiglesworth⁴³, D. J. Wilbern¹²³, H. G. Wilkens³⁷, J. J. H. Wilkinson³³, D. M. Williams⁴², H. H. Williams¹³¹, S. Williams³³, S. Willocq¹⁰⁵, B. J. Wilson¹⁰³, P. J. Windischhofer⁴⁰, F. I. Winkel³¹, F. Winkelmeier¹²⁶, B. T. Winter⁵⁵, J. K. Winter¹⁰³, M. Wittgen¹⁴⁷, M. Wobisch⁹⁹, T. Wojtkowski⁶¹, Z. Wolffs¹¹⁷, J. Wollrath¹⁶², M. W. Wolter⁸⁸, H. Wolters^{133a,133c}, M. C. Wong¹³⁹, E. L. Woodward⁴², S. D. Worm⁴⁹, B. K. Wosiek⁸⁸, K. W. Woźniak⁸⁸, S. Wozniowski⁵⁶, K. Wright⁶⁰, C. Wu²¹, M. Wu^{114b}, M. Wu¹¹⁶, S. L. Wu¹⁷³, X. Wu⁵⁷, Y. Wu^{63a}, Z. Wu⁴, J. Wuerzinger^{112,ad}, T. R. Wyatt¹⁰³, B. M. Wynne⁵³, S. Xella⁴³, L. Xia^{114a}, M. Xia¹⁵, M. Xie^{63a}, S. Xin^{14,114c}, A. Xiong¹²⁶, J. Xiong^{18a}, D. Xu¹⁴, H. Xu^{63a}, L. Xu^{63a}, R. Xu¹³¹, T. Xu¹⁰⁸, Y. Xu¹⁵, Z. Xu⁵³, Z. Xu^{114a}, B. Yabsley¹⁵¹, S. Yacob^{34a}, Y. Yamaguchi⁸⁵, E. Yamashita¹⁵⁷, H. Yamauchi¹⁶⁰, T. Yamazaki^{18a}, Y. Yamazaki⁸⁶, J. Yan^{63c}, S. Yan⁶⁰, Z. Yan¹⁰⁵, H. J. Yang^{63c,63d}, H. T. Yang^{63a}, S. Yang^{63a}, T. Yang^{65c}, X. Yang³⁷, X. Yang¹⁴, Y. Yang⁴⁵, Y. Yang^{63a}, Z. Yang^{63a}, W.-M. Yao^{18a}, H. Ye^{114a}, H. Ye⁵⁶, J. Ye¹⁴, S. Ye³⁰, X. Ye^{63a}, Y. Yeh⁹⁸, I. Yeletskikh³⁹, B. Yeo^{18b}, M. R. Yexley⁹⁸, T. P. Yildirim¹²⁹, P. Yin⁴², K. Yorita¹⁷¹, S. Younas^{28b}, C. J. S. Young³⁷, C. Young¹⁴⁷, C. Yu^{14,114c}, Y. Yu^{63a}, J. Yuan^{14,114c}, M. Yuan¹⁰⁸, R. Yuan^{63c,63d}, L. Yue⁹⁸, M. Zaazoua^{63a}, B. Zabinski⁸⁸, E. Zaid⁵³, Z. K. Zak⁸⁸, T. Zakareishvili¹⁶⁶, S. Zambito⁵⁷, J. A. Zamora Saa^{140b,140d}, J. Zang¹⁵⁷, D. Zanzi⁵⁵

O. Zaplatilek¹³⁵ , C. Zeitnitz¹⁷⁴ , H. Zeng¹⁴ , J. C. Zeng¹⁶⁵ , D. T. Zenger Jr.²⁷ , O. Zenin³⁸ , T. Ženiš^{29a} , S. Zenz⁹⁶ , S. Zerradi^{36a} , D. Zerwas⁶⁷ , M. Zhai^{14,114c} , D. F. Zhang¹⁴³ , J. Zhang^{63b} , J. Zhang⁶ , K. Zhang^{14,114c} , L. Zhang^{63a} , L. Zhang^{114a} , P. Zhang^{14,114c} , R. Zhang¹⁷³ , S. Zhang¹⁰⁸ , S. Zhang⁹¹ , T. Zhang¹⁵⁷ , X. Zhang^{63c} , X. Zhang^{63b} , Y. Zhang^{63c} , Y. Zhang⁹⁸ , Y. Zhang^{114a} , Z. Zhang^{18a} , Z. Zhang^{63b} , Z. Zhang⁶⁷ , H. Zhao¹⁴² , T. Zhao^{63b} , Y. Zhao¹³⁹ , Z. Zhao^{63a} , Z. Zhao^{63a} , A. Zhemchugov³⁹ , J. Zheng^{114a} , K. Zheng¹⁶⁵ , X. Zheng^{63a} , Z. Zheng¹⁴⁷ , D. Zhong¹⁶⁵ , B. Zhou¹⁰⁸ , H. Zhou⁷ , N. Zhou^{63c} , Y. Zhou¹⁵ , Y. Zhou^{114a} , Y. Zhou⁷ , C. G. Zhu^{63b} , J. Zhu¹⁰⁸ , X. Zhu^{63d} , Y. Zhu^{63c} , Y. Zhu^{63a} , X. Zhuang¹⁴ , K. Zhukov⁶⁹ , N. I. Zimine³⁹ , J. Zinsser^{64b} , M. Ziolkowski¹⁴⁵ , L. Živković¹⁶ , A. Zoccoli^{24a,24b} , K. Zoch⁶² , T. G. Zorbas¹⁴³ , O. Zormpa⁴⁷ , W. Zou⁴² , L. Zwaliński³⁷

¹ Department of Physics, University of Adelaide, Adelaide, Australia

² Department of Physics, University of Alberta, Edmonton, AB, Canada

³ ^(a)Department of Physics, Ankara University, Ankara, Türkiye; ^(b)Division of Physics, TOBB University of Economics and Technology, Ankara, Türkiye

⁴ LAPP, Université Savoie Mont Blanc, CNRS/IN2P3, Annecy, France

⁵ APC, Université Paris Cité, CNRS/IN2P3, Paris, France

⁶ High Energy Physics Division, Argonne National Laboratory, Argonne, IL, USA

⁷ Department of Physics, University of Arizona, Tucson, AZ, USA

⁸ Department of Physics, University of Texas at Arlington, Arlington, TX, USA

⁹ Physics Department, National and Kapodistrian University of Athens, Athens, Greece

¹⁰ Physics Department, National Technical University of Athens, Zografou, Greece

¹¹ Department of Physics, University of Texas at Austin, Austin, TX, USA

¹² Institute of Physics, Azerbaijan Academy of Sciences, Baku, Azerbaijan

¹³ Institut de Física d'Altes Energies (IFAE), Barcelona Institute of Science and Technology, Barcelona, Spain

¹⁴ Institute of High Energy Physics, Chinese Academy of Sciences, Beijing, China

¹⁵ Physics Department, Tsinghua University, Beijing, China

¹⁶ Institute of Physics, University of Belgrade, Belgrade, Serbia

¹⁷ Department for Physics and Technology, University of Bergen, Bergen, Norway

¹⁸ ^(a)Physics Division, Lawrence Berkeley National Laboratory, Berkeley, CA, USA; ^(b)University of California, Berkeley, CA, USA

¹⁹ Institut für Physik, Humboldt Universität zu Berlin, Berlin, Germany

²⁰ Albert Einstein Center for Fundamental Physics and Laboratory for High Energy Physics, University of Bern, Bern, Switzerland

²¹ School of Physics and Astronomy, University of Birmingham, Birmingham, UK

²² ^(a)Department of Physics, Bogazici University, Istanbul, Türkiye; ^(b)Department of Physics Engineering, Gaziantep University, Gaziantep, Türkiye; ^(c)Department of Physics, Istanbul University, Istanbul, Türkiye

²³ ^(a)Facultad de Ciencias y Centro de Investigaciones, Universidad Antonio Nariño, Bogotá, Colombia; ^(b)Departamento de Física, Universidad Nacional de Colombia, Bogotá, Colombia

²⁴ ^(a)Dipartimento di Fisica e Astronomia A. Righi, Università di Bologna, Bologna, Italy; ^(b)INFN Sezione di Bologna, Bologna, Italy

²⁵ Physikalischs Institut, Universität Bonn, Bonn, Germany

²⁶ Department of Physics, Boston University, Boston, MA, USA

²⁷ Department of Physics, Brandeis University, Waltham, MA, USA

²⁸ ^(a)Transilvania University of Brasov, Brasov, Romania; ^(b)Horia Hulubei National Institute of Physics and Nuclear Engineering, Bucharest, Romania; ^(c)Department of Physics, Alexandru Ioan Cuza University of Iasi, Iasi, Romania; ^(d)Physics Department, National Institute for Research and Development of Isotopic and Molecular Technologies, Cluj-Napoca, Romania; ^(e)National University of Science and Technology Politehnica, Bucharest, Romania; ^(f)West University in Timisoara, Timisoara, Romania; ^(g)Faculty of Physics, University of Bucharest, Bucharest, Romania

²⁹ ^(a)Faculty of Mathematics, Physics and Informatics, Comenius University, Bratislava, Slovakia; ^(b)Department of Subnuclear Physics, Institute of Experimental Physics of the Slovak Academy of Sciences, Kosice, Slovak Republic

³⁰ Physics Department, Brookhaven National Laboratory, Upton, NY, USA

- ³¹ Universidad de Buenos Aires, Facultad de Ciencias Exactas y Naturales, Departamento de Física, y CONICET, Instituto de Física de Buenos Aires (IFIBA), Buenos Aires, Argentina
- ³² California State University, CA, USA
- ³³ Cavendish Laboratory, University of Cambridge, Cambridge, UK
- ³⁴ ^(a)Department of Physics, University of Cape Town, Cape Town, South Africa; ^(b)iThemba Labs, Cape Town, Western Cape, South Africa; ^(c)Department of Mechanical Engineering Science, University of Johannesburg, Johannesburg, South Africa; ^(d)National Institute of Physics, University of the Philippines Diliman (Philippines), Quezon City, Philippines; ^(e)Department of Physics, University of South Africa, Pretoria, South Africa; ^(f)University of Zululand, KwaDlangezwa, South Africa; ^(g)School of Physics, University of the Witwatersrand, Johannesburg, South Africa
- ³⁵ Department of Physics, Carleton University, Ottawa, ON, Canada
- ³⁶ ^(a)Faculté des Sciences Ain Chock, Université Hassan II de Casablanca, Casablanca, Morocco; ^(b)Faculté des Sciences, Université Ibn-Tofail, Kénitra, Morocco; ^(c)Faculté des Sciences Semlalia, Université Cadi Ayyad, LPHEA, Marrakech, Morocco; ^(d)LPMR, Faculté des Sciences, Université Mohamed Premier, Oujda, Morocco; ^(e)Faculté des sciences, Université Mohammed V, Rabat, Morocco; ^(f)Institute of Applied Physics, Mohammed VI Polytechnic University, Ben Guerir, Morocco
- ³⁷ CERN, Geneva, Switzerland
- ³⁸ Affiliated with an Institute Covered by a Cooperation Agreement with CERN, Geneva, Switzerland
- ³⁹ Affiliated with an International Laboratory Covered by a Cooperation Agreement with CERN, Geneva, Switzerland
- ⁴⁰ Enrico Fermi Institute, University of Chicago, Chicago, IL, USA
- ⁴¹ LPC, Université Clermont Auvergne, CNRS/IN2P3, Clermont-Ferrand, France
- ⁴² Nevis Laboratory, Columbia University, Irvington, NY, USA
- ⁴³ Niels Bohr Institute, University of Copenhagen, Copenhagen, Denmark
- ⁴⁴ ^(a)Dipartimento di Fisica, Università della Calabria, Rende, Italy; ^(b)INFN Gruppo Collegato di Cosenza, Laboratori Nazionali di Frascati, Frascati, Italy
- ⁴⁵ Physics Department, Southern Methodist University, Dallas, TX, USA
- ⁴⁶ Physics Department, University of Texas at Dallas, Richardson, TX, USA
- ⁴⁷ National Centre for Scientific Research “Demokritos”, Agia Paraskevi, Greece
- ⁴⁸ ^(a)Department of Physics, Stockholm University, Stockholm, Sweden; ^(b)Oskar Klein Centre, Stockholm, Sweden
- ⁴⁹ Deutsches Elektronen-Synchrotron DESY, Hamburg and Zeuthen, Germany
- ⁵⁰ Fakultät Physik, Technische Universität Dortmund, Dortmund, Germany
- ⁵¹ Institut für Kern- und Teilchenphysik, Technische Universität Dresden, Dresden, Germany
- ⁵² Department of Physics, Duke University, Durham, NC, USA
- ⁵³ SUPA-School of Physics and Astronomy, University of Edinburgh, Edinburgh, UK
- ⁵⁴ INFN e Laboratori Nazionali di Frascati, Frascati, Italy
- ⁵⁵ Physikalischs Institut, Albert-Ludwigs-Universität Freiburg, Freiburg, Germany
- ⁵⁶ II. Physikalischs Institut, Georg-August-Universität Göttingen, Göttingen, Germany
- ⁵⁷ Département de Physique Nucléaire et Corpusculaire, Université de Genève, Geneva, Switzerland
- ⁵⁸ ^(a)Dipartimento di Fisica, Università di Genova, Genoa, Italy; ^(b)INFN Sezione di Genova, Genoa, Italy
- ⁵⁹ II. Physikalischs Institut, Justus-Liebig-Universität Giessen, Giessen, Germany
- ⁶⁰ SUPA-School of Physics and Astronomy, University of Glasgow, Glasgow, UK
- ⁶¹ LPSC, Université Grenoble Alpes, CNRS/IN2P3, Grenoble INP, Grenoble, France
- ⁶² Laboratory for Particle Physics and Cosmology, Harvard University, Cambridge, MA, USA
- ⁶³ ^(a)Department of Modern Physics and State Key Laboratory of Particle Detection and Electronics, University of Science and Technology of China, Hefei, China; ^(b)Institute of Frontier and Interdisciplinary Science and Key Laboratory of Particle Physics and Particle Irradiation (MOE), Shandong University, Qingdao, China; ^(c)State Key Laboratory of Dark Matter Physics, School of Physics and Astronomy, Shanghai Jiao Tong University, Key Laboratory for Particle Astrophysics and Cosmology (MOE), SKLPPC, Shanghai, China; ^(d)State Key Laboratory of Dark Matter Physics, Tsung-Dao Lee Institute, Shanghai Jiao Tong University, Shanghai, China; ^(e)School of Physics, Zhengzhou University, Zhengzhou, China
- ⁶⁴ ^(a)Kirchhoff-Institut für Physik, Ruprecht-Karls-Universität Heidelberg, Heidelberg, Germany; ^(b)Physikalischs Institut, Ruprecht-Karls-Universität Heidelberg, Heidelberg, Germany

- ⁶⁵ ^(a)Department of Physics, Chinese University of Hong Kong, Shatin, N.T., Hong Kong; ^(b)Department of Physics, University of Hong Kong, Hong Kong; ^(c)Department of Physics and Institute for Advanced Study, Hong Kong University of Science and Technology, Clear Water Bay, Kowloon, Hong Kong, China
- ⁶⁶ Department of Physics, National Tsing Hua University, Hsinchu, Taiwan
- ⁶⁷ IJCLab, Université Paris-Saclay, CNRS/IN2P3, 91405 Orsay, France
- ⁶⁸ Centro Nacional de Microelectrónica (IMB-CNM-CSIC), Barcelona, Spain
- ⁶⁹ Department of Physics, Indiana University, Bloomington, IN, USA
- ⁷⁰ ^(a)INFN Gruppo Collegato di Udine, Sezione di Trieste, Udine, Italy; ^(b)ICTP, Trieste, Italy; ^(c)Dipartimento Politecnico di Ingegneria e Architettura, Università di Udine, Udine, Italy
- ⁷¹ ^(a)INFN Sezione di Lecce, Lecce, Italy; ^(b)Dipartimento di Matematica e Fisica, Università del Salento, Lecce, Italy
- ⁷² ^(a)INFN Sezione di Milano, Milan, Italy; ^(b)Dipartimento di Fisica, Università di Milano, Milan, Italy
- ⁷³ ^(a)INFN Sezione di Napoli, Naples, Italy; ^(b)Dipartimento di Fisica, Università di Napoli, Naples, Italy
- ⁷⁴ ^(a)INFN Sezione di Pavia, Pavia, Italy; ^(b)Dipartimento di Fisica, Università di Pavia, Pavia, Italy
- ⁷⁵ ^(a)INFN Sezione di Pisa, Pisa, Italy; ^(b)Dipartimento di Fisica E. Fermi, Università di Pisa, Pisa, Italy
- ⁷⁶ ^(a)INFN Sezione di Roma, Rome, Italy; ^(b)Dipartimento di Fisica, Sapienza Università di Roma, Rome, Italy
- ⁷⁷ ^(a)INFN Sezione di Roma Tor Vergata, Rome, Italy; ^(b)Dipartimento di Fisica, Università di Roma Tor Vergata, Rome, Italy
- ⁷⁸ ^(a)INFN Sezione di Roma Tre, Rome, Italy; ^(b)Dipartimento di Matematica e Fisica, Università Roma Tre, Rome, Italy
- ⁷⁹ ^(a)INFN-TIFPA, Povo, Italy; ^(b)Università degli Studi di Trento, Trento, Italy
- ⁸⁰ Universität Innsbruck, Department of Astro and Particle Physics, Innsbruck, Austria
- ⁸¹ University of Iowa, Iowa City, IA, USA
- ⁸² Department of Physics and Astronomy, Iowa State University, Ames, IA, USA
- ⁸³ Istinye University, Sarıyer, İstanbul, Türkiye
- ⁸⁴ ^(a)Departamento de Engenharia Elétrica, Universidade Federal de Juiz de Fora (UFJF), Juiz de Fora, Brazil; ^(b)Universidade Federal do Rio De Janeiro COPPE/EE/IF, Rio de Janeiro, Brazil; ^(c)Instituto de Física, Universidade de São Paulo, São Paulo, Brazil; ^(d)Rio de Janeiro State University, Rio de Janeiro, Brazil; ^(e)Federal University of Bahia, Bahia, Brazil
- ⁸⁵ KEK, High Energy Accelerator Research Organization, Tsukuba, Japan
- ⁸⁶ Graduate School of Science, Kobe University, Kobe, Japan
- ⁸⁷ ^(a)AGH University of Krakow, Faculty of Physics and Applied Computer Science, Krakow, Poland; ^(b)Marian Smoluchowski Institute of Physics, Jagiellonian University, Krakow, Poland
- ⁸⁸ Institute of Nuclear Physics Polish Academy of Sciences, Krakow, Poland
- ⁸⁹ Faculty of Science, Kyoto University, Kyoto, Japan
- ⁹⁰ Research Center for Advanced Particle Physics and Department of Physics, Kyushu University, Fukuoka , Japan
- ⁹¹ L2IT, Université de Toulouse, CNRS/IN2P3, UPS, Toulouse, France
- ⁹² Instituto de Física La Plata, Universidad Nacional de La Plata and CONICET, La Plata, Argentina
- ⁹³ Physics Department, Lancaster University, Lancaster, UK
- ⁹⁴ Oliver Lodge Laboratory, University of Liverpool, Liverpool, UK
- ⁹⁵ Department of Experimental Particle Physics, Jožef Stefan Institute and Department of Physics, University of Ljubljana, Ljubljana, Slovenia
- ⁹⁶ Department of Physics and Astronomy, Queen Mary University of London, London, UK
- ⁹⁷ Department of Physics, Royal Holloway University of London, Egham, UK
- ⁹⁸ Department of Physics and Astronomy, University College London, London, UK
- ⁹⁹ Louisiana Tech University, Ruston, LA, USA
- ¹⁰⁰ Fysiska institutionen, Lunds universitet, Lund, Sweden
- ¹⁰¹ Departamento de Física Teórica C-15 and CIAFF, Universidad Autónoma de Madrid, Madrid, Spain
- ¹⁰² Institut für Physik, Universität Mainz, Mainz, Germany
- ¹⁰³ School of Physics and Astronomy, University of Manchester, Manchester, UK
- ¹⁰⁴ CPPM, Aix-Marseille Université, CNRS/IN2P3, Marseille, France
- ¹⁰⁵ Department of Physics, University of Massachusetts, Amherst, MA, USA
- ¹⁰⁶ Department of Physics, McGill University, Montreal, QC, Canada
- ¹⁰⁷ School of Physics, University of Melbourne, Melbourne, VIC, Australia
- ¹⁰⁸ Department of Physics, University of Michigan, Ann Arbor, MI, USA

- ¹⁰⁹ Department of Physics and Astronomy, Michigan State University, East Lansing, MI, USA
¹¹⁰ Group of Particle Physics, University of Montreal, Montreal, QC, Canada
¹¹¹ Fakultät für Physik, Ludwig-Maximilians-Universität München, Munich, Germany
¹¹² Max-Planck-Institut für Physik (Werner-Heisenberg-Institut), Munich, Germany
¹¹³ Graduate School of Science and Kobayashi-Maskawa Institute, Nagoya University, Nagoya, Japan
¹¹⁴ ^(a)Department of Physics, Nanjing University, Nanjing, China; ^(b)School of Science, Shenzhen Campus of Sun Yat-sen University, Shenzhen, China; ^(c)University of Chinese Academy of Science (UCAS), Beijing, China
¹¹⁵ Department of Physics and Astronomy, University of New Mexico, Albuquerque, NM, USA
¹¹⁶ Institute for Mathematics, Astrophysics and Particle Physics, Radboud University/Nikhef, Nijmegen, The Netherlands
¹¹⁷ Nikhef National Institute for Subatomic Physics and University of Amsterdam, Amsterdam, The Netherlands
¹¹⁸ Department of Physics, Northern Illinois University, DeKalb, IL, USA
¹¹⁹ ^(a)New York University Abu Dhabi, Abu Dhabi, United Arab Emirates; ^(b)United Arab Emirates University, Al Ain, United Arab Emirates
¹²⁰ Department of Physics, New York University, New York, NY, USA
¹²¹ Ochanomizu University, Otsuka, Bunkyo-ku, Tokyo, Japan
¹²² Ohio State University, Columbus, OH, USA
¹²³ Homer L. Dodge Department of Physics and Astronomy, University of Oklahoma, Norman, OK, USA
¹²⁴ Department of Physics, Oklahoma State University, Stillwater, OK, USA
¹²⁵ Palacký University, Joint Laboratory of Optics, Olomouc, Czech Republic
¹²⁶ Institute for Fundamental Science, University of Oregon, Eugene, OR, USA
¹²⁷ Graduate School of Science, Osaka University, Osaka, Japan
¹²⁸ Department of Physics, University of Oslo, Oslo, Norway
¹²⁹ Department of Physics, Oxford University, Oxford, UK
¹³⁰ LPNHE, Sorbonne Université, Université Paris Cité, CNRS/IN2P3, Paris, France
¹³¹ Department of Physics, University of Pennsylvania, Philadelphia, PA, USA
¹³² Department of Physics and Astronomy, University of Pittsburgh, Pittsburgh, PA, USA
¹³³ ^(a)Laboratório de Instrumentação e Física Experimental de Partículas-LIP, Lisbon, Portugal; ^(b)Departamento de Física, Faculdade de Ciências, Universidade de Lisboa, Lisbon, Portugal; ^(c)Departamento de Física, Universidade de Coimbra, Coimbra, Portugal; ^(d)Centro de Física Nuclear da Universidade de Lisboa, Lisbon, Portugal; ^(e)Departamento de Física, Escola de Ciências, Universidade do Minho, Braga, Portugal; ^(f)Departamento de Física Teórica y del Cosmos, Universidad de Granada, Granada, Spain; ^(g)Departamento de Física, Instituto Superior Técnico, Universidade de Lisboa, Lisbon, Portugal
¹³⁴ Institute of Physics of the Czech Academy of Sciences, Prague, Czech Republic
¹³⁵ Czech Technical University in Prague, Prague, Czech Republic
¹³⁶ Faculty of Mathematics and Physics, Charles University, Prague, Czech Republic
¹³⁷ Particle Physics Department, Rutherford Appleton Laboratory, Didcot, UK
¹³⁸ IRFU, CEA, Université Paris-Saclay, Gif-sur-Yvette, France
¹³⁹ Santa Cruz Institute for Particle Physics, University of California Santa Cruz, Santa Cruz, CA, USA
¹⁴⁰ ^(a)Departamento de Física, Pontificia Universidad Católica de Chile, Santiago, Chile; ^(b)Millennium Institute for Subatomic physics at high energy frontier (SAPHIR), Santiago, Chile; ^(c)Instituto de Investigación Multidisciplinario en Ciencia y Tecnología y Departamento de Física, Universidad de La Serena, La Serena, Chile; ^(d)Department of Physics, Universidad Andres Bello, Santiago, Chile; ^(e)Instituto de Alta Investigación, Universidad de Tarapacá, Arica, Chile; ^(f)Departamento de Física, Universidad Técnica Federico Santa María, Valparaíso, Chile
¹⁴¹ Department of Physics, Institute of Science, Tokyo, Japan
¹⁴² Department of Physics, University of Washington, Seattle, WA, USA
¹⁴³ Department of Physics and Astronomy, University of Sheffield, Sheffield, UK
¹⁴⁴ Department of Physics, Shinshu University, Nagano, Japan
¹⁴⁵ Department Physik, Universität Siegen, Siegen, Germany
¹⁴⁶ Department of Physics, Simon Fraser University, Burnaby, BC, Canada
¹⁴⁷ SLAC National Accelerator Laboratory, Stanford, CA, USA
¹⁴⁸ Department of Physics, Royal Institute of Technology, Stockholm, Sweden
¹⁴⁹ Departments of Physics and Astronomy, Stony Brook University, Stony Brook, NY, USA
¹⁵⁰ Department of Physics and Astronomy, University of Sussex, Brighton, UK

- ¹⁵¹ School of Physics, University of Sydney, Sydney, Australia
¹⁵² Institute of Physics, Academia Sinica, Taipei, Taiwan
¹⁵³ ^(a)E. Andronikashvili Institute of Physics, Iv. Javakhishvili Tbilisi State University, Tbilisi, Georgia; ^(b)High Energy Physics Institute, Tbilisi State University, Tbilisi, Georgia; ^(c)University of Georgia, Tbilisi, Georgia
¹⁵⁴ Department of Physics, Technion, Israel Institute of Technology, Haifa, Israel
¹⁵⁵ Raymond and Beverly Sackler School of Physics and Astronomy, Tel Aviv University, Tel Aviv, Israel
¹⁵⁶ Department of Physics, Aristotle University of Thessaloniki, Thessaloniki, Greece
¹⁵⁷ International Center for Elementary Particle Physics and Department of Physics, University of Tokyo, Tokyo, Japan
¹⁵⁸ Department of Physics, University of Toronto, Toronto, ON, Canada
¹⁵⁹ ^(a)TRIUMF, Vancouver, BC, Canada; ^(b)Department of Physics and Astronomy, York University, Toronto, ON, Canada
¹⁶⁰ Division of Physics and Tomonaga Center for the History of the Universe, Faculty of Pure and Applied Sciences, University of Tsukuba, Tsukuba, Japan
¹⁶¹ Department of Physics and Astronomy, Tufts University, Medford, MA, USA
¹⁶² Department of Physics and Astronomy, University of California Irvine, Irvine, CA, USA
¹⁶³ University of Sharjah, Sharjah, United Arab Emirates
¹⁶⁴ Department of Physics and Astronomy, University of Uppsala, Uppsala, Sweden
¹⁶⁵ Department of Physics, University of Illinois, Urbana, IL, USA
¹⁶⁶ Instituto de Física Corpuscular (IFIC), Centro Mixto Universidad de Valencia-CSIC, Valencia, Spain
¹⁶⁷ Department of Physics, University of British Columbia, Vancouver, BC, Canada
¹⁶⁸ Department of Physics and Astronomy, University of Victoria, Victoria, BC, Canada
¹⁶⁹ Fakultät für Physik und Astronomie, Julius-Maximilians-Universität Würzburg, Würzburg, Germany
¹⁷⁰ Department of Physics, University of Warwick, Coventry, UK
¹⁷¹ Waseda University, Tokyo, Japan
¹⁷² Department of Particle Physics and Astrophysics, Weizmann Institute of Science, Rehovot, Israel
¹⁷³ Department of Physics, University of Wisconsin, Madison, WI, USA
¹⁷⁴ Fakultät für Mathematik und Naturwissenschaften, Fachgruppe Physik, Bergische Universität Wuppertal, Wuppertal, Germany
¹⁷⁵ Department of Physics, Yale University, New Haven, CT, USA

^a Also Affiliated with an Institute Covered by a Cooperation Agreement with CERN, Geneva, Switzerland

^b Also at An-Najah National University, Nablus, Palestine

^c Also at Borough of Manhattan Community College, City University of New York, New York, NY, USA

^d Also at Center for High Energy Physics, Peking University, Beijing, China

^e Also at Center for Interdisciplinary Research and Innovation (CIRI-AUTH), Thessaloniki, Greece

^f Also at Centro Studi e Ricerche Enrico Fermi, Rome, Italy

^g Also at CERN, Geneva, Switzerland

^h Also at CMD-AC UNEC Research Center, Azerbaijan State University of Economics (UNEC), Baku, Azerbaijan

ⁱ Also at Département de Physique Nucléaire et Corpusculaire, Université de Genève, Geneva, Switzerland

^j Also at Departament de Física de la Universitat Autònoma de Barcelona, Barcelona, Spain

^k Also at Department of Financial and Management Engineering, University of the Aegean, Chios, Greece

^l Also at Department of Physics, California State University, Sacramento, USA

^m Also at Department of Physics, King's College London, London, UK

ⁿ Also at Department of Physics, Stanford University, Stanford, CA, USA

^o Also at Department of Physics, Stellenbosch University, Stellenbosch, South Africa

^p Also at Department of Physics, University of Fribourg, Fribourg, Switzerland

^q Also at Department of Physics, University of Thessaly, Volos, Greece

^r Also at Department of Physics, Westmont College, Santa Barbara, USA

^s Also at Faculty of Physics, Sofia University, ‘St. Kliment Ohridski’, Sofia, Bulgaria

^t Also at Hellenic Open University, Patras, Greece

^u Also at Institutio Catalana de Recerca i Estudis Avancats, ICREA, Barcelona, Spain

^v Also at Institut für Experimentalphysik, Universität Hamburg, Hamburg, Germany

^w Also at Institute for Nuclear Research and Nuclear Energy (INRNE) of the Bulgarian Academy of Sciences, Sofia, Bulgaria

^x Also at Institute of Applied Physics, Mohammed VI Polytechnic University, Ben Guerir, Morocco

^y Also at Institute of Particle Physics (IPP), Victoria, Canada

^z Also at Institute of Physics and Technology, Mongolian Academy of Sciences, Ulaanbaatar, Mongolia

^{aa} Also at Institute of Physics, Azerbaijan Academy of Sciences, Baku, Azerbaijan

^{ab} Also at Institute of Theoretical Physics, Ilia State University, Tbilisi, Georgia

^{ac} Also at National Institute of Physics, University of the Philippines Diliman (Philippines), Quezon City, Philippines

^{ad} Also at Technical University of Munich, Munich, Germany

^{ae} Also at The Collaborative Innovation Center of Quantum Matter (CICQM), Beijing, China

^{af} Also at TRIUMF, Vancouver, BC, Canada

^{ag} Also at Università di Napoli Parthenope, Naples, Italy

^{ah} Also at University of Colorado Boulder, Department of Physics, Colorado, USA

^{ai} Also at Washington College, Chestertown, MD, USA

^{aj} Also at Yeditepe University, Physics Department, Istanbul, Türkiye

* Deceased